

謹
呈

Thermal regime of a glacier in relation to
glacier ice formation

白
岩
孝
行
様

Thesis submitted
for Doctoral degree
by

Hisashi OZAWA

Institute of Low Temperature Science,
Hokkaido University
Sapporo

1991

著
者

ABSTRACT

In order to investigate thermal regime and stratigraphic conditions of a glacier, field observations were carried out on the Yala Glacier in the Nepal Himalaya. The results show that upper part of this glacier is temperate (temperature is at the melting point) throughout while its lower part is cold (below the melting point) and frozen to the bed rock. We call this glacier the inversion type glacier against the previous categories such as temperate and sub-polar. To clarify the cause of occurrence of the inversion type glacier, we investigate percolation process of meltwater into surface firn layer and formation process of the superimposed ice due to refreezing of this water. The results, obtained from this case study, are generalized for glaciers in the world, and a method is presented to classify glaciers into one of three typical types: temperate, cold and inversion types.

The findings are summarized as follows:

- (1) The inversion type glaciers, which are in disagreement with previous classification such as temperate or sub-polar glaciers, are widely distributed in the world.
- (2) The inversion type glacier has a temperate firn area (the temperate infiltration zone) where the firn temperature is at the melting point throughout in the upper part, and has a cold ice area (the superimposed-ice zone and the cold ablation zone) where the ice temperature is negative in the lower part.
- (3) The inversion type glacier can be found in the regions where winter is cold (the freezing index exceeds 2000°C day) and annual precipitation is more than 700 (mmH₂O).

(4) The temperate type glacier can be found in the regions where freezing index is less than 2000 ($^{\circ}\text{C day}$), while the cold type glacier can be found in the area where freezing index exceeds 2000 ($^{\circ}\text{C day}$) and annual precipitation is less than 700 (mmH_2O).

(5) The inversion type glacier is in a potentially unstable condition, because the upper mobile temperate ice is dammed up by the lower cold ice frozen to the bed rock. This instability can produce a rapid advance of the glacier, i.e., the glacier surge.

CONTENTS

| | | |
|------|--|----|
| 1. | INTRODUCTION | |
| 1-1. | Previous investigations | 5 |
| 1-2. | The inversion type glacier | 6 |
| 1-3. | Purposes of this study | 7 |
| 2. | FIELD OBSERVATIONS ON THE YALA GLACIER, NEPAL HIMALAYA | |
| 2-1. | Site description | 9 |
| 2-2. | Results of observations | 10 |
| 3. | CRITERIA FOR EACH ZONE BOUNDARY | |
| 3-1. | Temperate condition of firn area | 14 |
| 3-2. | Condition of superimposed ice formation | 17 |
| 3-3. | Temperate and cold ablation zone | 19 |
| 4. | ESTIMATION OF ZONES ON THE YALA GLACIER | |
| 4-1. | Estimation of surface balance and infiltration water | 21 |
| 4-2. | Estimation of internal accumulation | 23 |
| 4-3. | Zoning of the Yala Glacier | 26 |
| 5. | GENERAL CLASSIFICATION OF GLACIERS IN THE WORLD | |
| 5-1. | Generalized glacier zone model | 29 |
| 5-2. | Temperate, cold and inversion type glacier | 29 |
| 5-3. | General classification | 31 |
| 6. | DISCUSSION | |
| 6-1. | Effect of zone boundary on glacier flow | 34 |
| 6-2. | Instability of the inversion type glacier | 36 |
| 7. | CONCLUDING REMARKS | 38 |
| | ACKNOWLEDGMENTS | 39 |
| | APPENDIX I | 40 |
| | APPENDIX II | 42 |

| | |
|--------------|----|
| APPENDIX III | 43 |
| REFERENCES | 46 |
| TABLES | 52 |
| FIGURES | 55 |

1. INTRODUCTION

1-1. Previous investigations

In order to classify glaciers, Benson (1959) and Müller (1962) proposed the idea of glacier zones. According to Paterson (1981), a glacier can be divided into following five zones: *dry-snow zone*, *percolation zone*, *wet-snow zone*, *superimposed-ice zone* and *ablation zone* (Fig. 1). Their idea is, however, based on stratigraphic and thermal conditions at the uppermost annual snow layer near the glacier surface; it contains no information about deeper part of the glacier. Moreover, the location and extent of each zone on a glacier cannot be estimated.

On the other hand, whether temperature at the isothermal depth (usually 10-m depth temperature) is at the melting point (temperate) or below the melting point (cold) is important for glaciological investigations; such as, glacier flow (basal sliding and plastic deformation of glacier ice) and the densification process of snow into ice, because physical properties of snow and ice vary critically at the melting point. For these reasons, the Ahlmann's classification of *temperate* and *sub-polar* glacier (Ahlmann, 1935) is still used by several glaciologists. (A temperate glacier is at the melting point throughout. Temperature of a sub-polar glacier remains negative throughout except in the surface layer where meltwater percolates.) However, as many investigators pointed out, thermal conditions vary from one point on a glacier to another; very few glaciers can be fitted into a single category. We must, therefore, purpose to extend the idea of zones to a new one which is based on the thermal conditions at

the isothermal depth.

1-2. *The inversion type glacier*

Several glaciers are known to show "temperature inversion", i.e., firn temperature at and below the isothermal depth is "temperate" in the accumulation area, whereas ice temperature is "cold" in the ablation area. Air temperature is colder in the accumulation area than in the lower ablation area. Hence, glacier temperature at the isothermal depth is inverted against air temperature. We call this glacier *inversion type glacier*, which is in disagreement with the Ahlmann's classification of glaciers into temperate and sub-polar glaciers. Such a glacier is, however, found throughout the world, e.g., in the Himalaya (Watanabe et al., 1984; Tanaka et al., 1980), in the Alps (Lliboutry et al., 1976; Haeberli, 1976), in Scandinavia (Schytt, 1968), in the Canadian Rockies (Paterson, 1972), in Alaska (Harrison et al., 1975; Trabant et al., 1975) and in polar ice caps (Schytt, 1969; Loewe, 1966; Casassa, 1989). Table I shows some examples of the inversion type glaciers and climatic elements (air temperature and precipitation) estimated on each glacier. The climatic features for the inversion type glaciers are:

- (1) Annual mean air temperature is from -5 to -15°C .
- (2) In summer, air temperature rises above 0°C and surface melting occurs.
- (3) Annual precipitation is more than 500 ($\text{mmH}_2\text{O a}^{-1}$).

Thus, the inversion type glacier would be likely to appear in regions where winter is cold and considerable accumulation and

ablation both occur, although the reason is not yet clear.

Schytt (1969) pointed out that the inversion type glacier has a potential instability for glacier surge. Figure 2 is a schematic illustration of a vertical section of an ice cap in eastern Svalbard observed by Schytt. The main part of the ice mass is at the melting point, and this temperate ice is surrounded by a ring of cold ice frozen to the bed. If this cold ice "dam" happens to be broken, a rapid advance (the surge) will occur. His suggestion stimulated development of some thermal models for glacier surge (Clarke, 1976; Cary et al., 1979). However, still now, there remains no reasonable explanation of why such temperature inversions occur in some glaciers.

1-3. Purposes of this study

It has been obvious that the inversion type glacier, which deviates from previous classifications, is distributed widely in the world, and that it has potential instability for glacier surge. We will clarify the cause of occurrence of the inversion type glacier in the following way:

(1) We describe a new method to predict the location and extent of each glacier zone which is defined by the temperature conditions (temperate or cold) at the isothermal depth.

(2) By considering the possible combination of these zones under several specific climatic conditions, we propose three typical glacier types: inversion type, temperate type and cold type. (Temperate type and cold type correspond to previous temperate and sub-polar, respectively.)

(3) We describe a general method to classify glaciers into above three types according to air temperature and precipitation estimated on each glacier.

The Yala Glacier in Nepal Himalaya was selected for a case study. This glacier is known to be an inversion type glacier (Watanabe et al., 1984). We observed internal stratigraphy and temperature conditions of this glacier by means of core drilling in 1987 (Yamada, 1989). First, we divide this glacier into several zones by the thermal and stratigraphic conditions at the isothermal depth. Second, we present simple equations to estimate the location of each zone boundary, and confirm their applicability to this glacier. Finally, we extend our glacier zone model to a generalized one, and thereby clarify the relationship between three glacier types and climatic conditions. Our method is applicable to any glacier in the world, and can predict stratigraphic and thermal conditions in a glacier if climatic elements such as temperature and precipitation on the glacier are known.

2. FIELD OBSERVATIONS ON THE YALA GLACIER, NEPAL HIMALAYA

2-1. Site description

The Yala Glacier, a small ice cap type glacier with no debris covered area, is located at lat. 28°15'N, long. 85° 37'E in the Langtang Valley, in the central Nepal Himalaya (Fig. 3). It is about 1.5 km in length, its area is 2.6 km². Its altitude extends from 5090 m to 5600 m above sea level (a.s.l.). The snow line, the lower limit of firn area, was observed at 5210 m at the end of summer in 1987.

In the Himalayan regions, two typical types of glacier are known: (1) ice cap type glacier without debris covered area, such as the Yala Glacier; and (2) valley type glacier with thick debris covered area in its lower part, the terminus of which is 500-1000 m lower than that of the ice cap type (Fujii and Higuchi, 1977). The debris covered ice is considered to be a stagnant relic ice which had advanced in the Little Ice Age (Fushimi, 1978; Shiraiwa and Watanabe, to be published). We will discuss the cause of such advance in section 6-2.

The Yala Glacier is known to be a inversion type glacier. Two deep core drilling observations were carried out at Y4 (5200 m a.s.l.) just below the snow line in 1981 and at Y11 (5407 m a.s.l.) above the snow line in 1982 (Watanabe et al., 1984). Figure 4 shows the results obtained from their observations. At Y4, ice was exposed at the surface and the ice temperature from below the surface to the bottom (31 m in depth) was negative (about -1°C) throughout, and the ice bottom was frozen to the bed rock. At Y11, a thick firn layer existed from the sur-

face to a depth of 17 m, where firn changed into ice by self-compressive deformation in the wet condition (Iida et al., 1984). Temperature from the surface to the bottom (60 m in depth) was completely at the melting point. Hence, this glacier is temperate in the upper firn area and cold in the lower ice area, i.e., the inversion type.

In order to investigate how the thermal and stratigraphic conditions change from Y4 to Y11, we carried out shallow core-drilling observations at sites Y5, Y6, Y7, Y9, Y10, Y11 and Y12 (see Fig. 3-c) in late summer of 1987. Using core samples, we measured density, free water content, levels of dirt layer, levels and thicknesses of ice layer. We purpose to know internal stratigraphy and thermal conditions of an inversion type glacier in the Nepal Himalaya.

2-2. Results of observations

Sudden disappearance of the ice mass was observed at a surface altitude of 5270 m a.s.l. on the Yala Glacier. Figure 5 shows stratigraphy observed at each coring site. The black strip indicates ice layer or ice mass of which density exceeds $0.83 \text{ (Mg km}^{-3}\text{)}$. Above the snow line (5210 m) to Y7 (5269 m), the ice mass was buried under the firn layer. The continuous ice mass, however, disappeared and changed to discontinuous thick ice layers at Y9 (5304 m) in spite of only 35-m increase of altitude. At higher sites (Y10-Y12), only thin ice layers were observed in the firn layer. In order to confirm this stratigraphic change, we drilled twice at Y7 and Y9 as shown in Fig. 5 with the subscript

(a) and (b); the point (a) is 10 m away from point (b) in horizontal distance. We thereby confirmed that there is a distinct sub-surface stratigraphic boundary at the surface altitude of 5270 m.

In the area above this boundary, temperature of the firn layer, including thin ice layers, was completely at the melting point. The free water content of the firn, measured at Y9-a in September of 1987, was 0-5% from the surface to the depth of 13 m. Deep core-drilling observation, carried out at Y11 in 1982, showed that some water poured out from the wall of the hole at the depth of 25.5 m and it filled the hole up to the depth of 20 m (see Fig. 4; Watanabe et al., 1984). We also observed that some water flowed out from the hole-wall to the level of 12.3 m at Y9-a. Hence, we define the area above the boundary as the *temperate infiltration zone* where firn temperature is at the melting point throughout by late summer as a result of infiltration of meltwater (Shumskii, 1964; p. 420). In this zone, wet firn changes into ice by self-compressive deformation at the melting point (Wakahama, 1968); the firn-ice transition depth is about 20 m in this zone.

In the area below this boundary, the continuous ice mass exists near the surface and ice temperature is negative; this ice consists of superimposed ice. Deep core drilling observation, carried out at Y4 (5200 m) in 1981, showed that temperature of the glacier ice was negative (about -1°C) throughout and the bottom (30m in depth) was frozen to the bed rock (Watanabe et al., 1982). We also found negative temperature in the ice at Y7-a

because the drilling machine was often stuck by refreezing of wet slime. Since the firn layer on this ice is too thin (0-3 m) to form ice by self-compressive deformation, we believe that this ice is formed by refreezing of meltwater when the infiltrated water arrives at the surface of ice that has been cooled in the previous winter season. This is called superimposed ice (Wakahama et al., 1976). The ice temperature remains negative even at the end of summer as a result of its impermeability to water. We define this area below this stratigraphic boundary as *superimposed-ice zone*, where continuous mass of superimposed ice grows near the surface. In our definition, the superimposed-ice zone includes the area above the snow line; although Paterson (1981, p. 8) restricts it to the area below the snow line where superimposed ice is exposed at the surface by ablation at the end of summer.

Figure 3 illustrates the internal structure of the longitudinal section of the Yala Glacier. In general, firn temperature is more likely to be temperate than ice because meltwater can percolate into firn but cannot percolate into ice during summer, and winter coldness cannot penetrate deeply into wet firn but can penetrate into ice during winter. The temperature inversion is, therefore, caused by the stratigraphic difference of snow and ice at the boundary at the surface altitude of 5270 m. The problems to be solved are: (1) how the firn temperature can be temperate throughout in the cold climate region (annual mean air temperature, estimated on this glacier, is from -4 to -7°C, Table I); and (2) how continuous superimposed ice can be formed in the

lower part of the accumulation area. The causes will be discussed in the next sections (3-1. and 3-2.) by introducing two simple criteria.

A dirt layer, which shows early summer surface, is easily identified in cores as shown with dotted lines in Fig. 5. The layer, bounded by the dirt layers, means an annual layer and its mass in water equivalent represents net balance, which fairly increases with the increase of altitude. The amount of net balance, b_n ($\text{mmH}_2\text{O a}^{-1}$), during 1986-87 is listed in Table II.

3. CRITERIA FOR EACH ZONE BOUNDARY

3-1. *Temperate condition of firn area*

Firn temperature can be temperate throughout, when there is a large enough supply of meltwater into firn during summer. Hence, we will discuss freezing process and wetting process of firn during a year, and evaluate the conditions necessary for the firn layer to be temperate throughout. We initially assume a temperate condition: the firn is completely wet (at the melting point) in late summer. Then we estimate the amount of internal accumulation, $c_a(i)$, amount of water frozen by penetration of winter coldness, and discuss if the firn temperature can return to the initial wet condition by infiltration of meltwater, as follows.

We will set the initial condition at the wet condition (free water content of the firn is about 3 %) in late summer, as shown in Fig. 7-a. During winter, the winter coldness penetrates into the wet firn through heat conduction, and freezes the capillary water retained in the firn. If the depth of freezing reaches its maximum, D , at the end of winter (Fig. 7-b), then the winter term of internal accumulation, i.e., the amount of water frozen in winter, is given by,

$$c_w(i) = \int_0^D \omega \, dz \quad (1)$$

where ω is free water content per unit volume that was retained in firn at the beginning of winter and z is measured downward from the firn surface. (We use the symbol (i) for internal mass-

balance terms and (s) for surface mass-balance terms.) When summer comes, meltwater and rain water infiltrate into the cooled firn layer, and it freezes to ice layers and ice glands in the layer (Fig. 7-c). The latent heat, released through freezing, warms the firn temperature to the melting point. Thus, the summer term of internal accumulation, $c_s(i)$, (the amount of water frozen in the firn layer during summer) can be estimated by increase of heat content in this layer during summer:

$$c_s(i) = \frac{1}{L} \int_0^D \rho c(\theta_e - \theta_b) dz \quad (2)$$

where L is the latent heat of fusion of ice, ρ is the density of firn, c is the specific heat of ice, θ_e and θ_b are the firn temperature at the end of winter and at the beginning of winter, respectively.

The annual amount of internal accumulation, $c_a(i)$, is the sum of the winter term and the summer term:

$$c_a(i) = c_w(i) + c_s(i) \quad (3)$$

This amount reaches a maximum value, $c_a(i)^*$, when there is a large enough supply of infiltration water in summer and thereby the firn temperature returns to the initial melting point ($\theta_e=0$):

$$c_a(i)^* = \int_0^D \omega dz + \frac{1}{L} \int_0^D \rho c(-\theta_b) dz \quad (4)$$

If the supply of infiltration water, Q_a , is greater than

this maximum value ($c_a(i)^*$), then the firn temperature can be the melting point throughout, and free water content, ω , can return to the initial value (Fig. 7-d). (We neglect the amount of water trapped in the new snow.) This is the temperate condition:

$$Q_a > c_a(i)^* \quad (5)$$

The area which satisfies this equation can be temperate throughout by late summer, when there is no impermeable ice near the surface (i.e., superimposed ice). This area is the *temperate infiltration zone*. In this zone the maximum amount, $c_a(i)^*$, is accumulated in the firn layer as actual internal accumulation: $c_a(i) = c_a(i)^*$, and a part of infiltration water ($Q_a - c_a(i)$) is lost by runoff.

In the area where $Q_a < c_a(i)^*$ (usually this area is higher than the temperate infiltration zone), the temperature of the deeper firn layer remains negative even at the end of summer. In next winter, the wetted firn layer is completely frozen and the winter coldness intrudes deeper than the depth of previous winter. As the result of repeating of this process, the firn temperature becomes negative except for its surface layer where melt-water and rain water infiltrate in summer (Fig. 7-e). This area is the *cold infiltration zone* where the firn temperature at the isothermal depth is negative, and cold firn changes into ice by self-compressive deformation at negative temperature (Shumskii, 1964). The depth of firn-ice transition is 50 to 70 m (Paterson, 1981; p.15). In this zone, all infiltration water is trapped as internal accumulation: $c_a(i) = Q_a$, and there is no runoff.

As the above discussion shows, we can estimate the location of the zone boundary of the temperate infiltration zone and the cold infiltration zone by $Q_a = c_a(i)^*$: equation (5).

3-2. Condition of superimposed-ice formation

Density of snow and firn is increased by repeating of the annual internal accumulation (i.e., annual wetting and refreezing process). The annual density increase through refreezing is repeated for several years until the firn is buried deeper than the freezing depth, D . Figure 8 schematically shows the repeating process in a temperate infiltration zone. The amount of annual increase of density is approximately $c_a(i)/D$, and repeating year is D/d ; where d is the thickness of annual layer. Thus the total increase of firn density through refreezing, $\Delta\rho$, at the bottom of the freezing layer is given by,

$$\Delta\rho = \frac{c_a(i)}{D} \cdot \frac{D}{d} = \frac{c_a(i)}{d} \quad (6)$$

In the cold infiltration zone, we must replace the freezing depth, D , in the above equation by the maximum depth of wetting front by late summer. However, the total increase of density is independent of the depth, D . Equation (6) is, therefore, valid in both the temperate infiltration zone and the cold infiltration zone.

We can replace d in equation (6) by $b_a(s)/\rho_s$; where $b_a(s)$ is the annual surface balance and ρ_s is the average density of initial snow. (Here the symbol (s) denotes the surface mass-

balance term.) Then, the total increase of density by refreezing (i.e., amount of refreezing per unit volume of firn) is given by,

$$\Delta \rho = \frac{c_a(i)}{b_a(s)} \rho_s. \quad (7)$$

Equation (7) shows that $\Delta \rho$ is proportional to annual internal accumulation, $c_a(i)$, but is inversely proportional to annual surface balance, $b_a(s)$. As shown in section 4.2, $c_a(i)$ is nearly constant on a glacier. Hence, the effect of densification by refreezing is larger in the lower accumulation area where $b_a(s)$ is smaller.

If the firn density has exceeded the ice transition density (i.e., $\rho_s + \Delta \rho > \rho_i = 0.83 \text{ Mg m}^{-3}$) by refreezing, then the firn changes into impermeable ice within the freezing layer. (We have neglected the effect of compression of firn in this layer.) This is the criterion for formation of superimposed ice:

$$b_a(s) < \alpha c_a(i)$$

$$\alpha = \frac{\rho_s}{\rho_i - \rho_s} \quad (8)$$

where α is the parameter depending on initial snow density. For example, when ρ_s is from 0.45 to 0.5, α varies from 1.2 to 1.5. The area which satisfies above equation is the *superimposed-ice zone*. In this area, superimposed ice grows near the glacier surface, and the ice temperature remains negative even at the late summer as a result of its impermeability to water. Thus the

temperature at the isothermal depth is negative, even though the area satisfies the temperate condition (Eq. (5)).

In the area where $b_a(s) > \alpha c_a(i)$ (usually this area is higher than the superimposed-ice zone), only discontinuous ice layers can be formed in the freezing layer. The interlaminated firn layers change to ice by self-compressive deformation at the depth of 20 m; this is deeper than the freezing depth, D . When there is enough infiltration water (i.e., the temperate condition of Eq. (5) is satisfied), this area can be temperate: the temperate infiltration zone. In this case, with increasing altitude, the superimposed-ice zone changes to the temperate infiltration zone at the boundary where $b_a(s) = \alpha c_a(i)$. On the contrary, when there is not enough infiltration water (i.e., Eq.(5) is not satisfied), then this area belongs to the cold infiltration zone. In that case, the superimposed-ice zone directly changes to the cold infiltration zone at the boundary where $b_a(s) = \alpha c_a(i) = \alpha Q_a$. This difference corresponds to the difference between inversion type glaciers and cold type glaciers as discussed in section 5.2. We can use equation (8) to estimate the upper limit of the superimposed-ice zone, whether that area satisfies the temperate condition (Eq. (5)) or not.

3-3. Temperate and cold ablation zone

The lower boundary of the superimposed-ice zone is taken at the equilibrium line (Paterson, 1981; p. 8). The equilibrium line is given by,

$$b_a(s) + c_a(i) = 0. \quad (9)$$

The area above this boundary (i.e., $b_a(s) > -c_a(i)$ and $b_a(s) < \alpha c_a(i)$) is the superimposed-ice zone. Strictly speaking, in a very temperate climate region where winter is not cold (i.e., $c_a(i) = 0$), the superimposed-ice zone is absent; this is the temperate type glacier. However, as shown in section 5-2., very few glaciers belong to this category. All glaciers where winter is cold ($c_a(i) > 0$) should have a superimposed-ice zone above the equilibrium line.

The area below this boundary ($b_a(s) < -c_a(i)$) is the ablation area. We can divide this area into two zones: upper cold ablation zone and lower temperate ablation zone. In the cold ablation area, winter coldness remains in the ice mass even at the late summer as a result of its impermeability to water, and temperature at the isothermal depth is negative, while in the temperate ablation zone, winter coldness in the ice mass is depleted by ablation of ice itself (Paterson, 1972); temperature of the ice mass is completely at the melting point to the bottom by the late summer. The boundary between above two zones is given by,

$$b_a(s) + c_a(i) = -D \rho_i \quad (10)$$

In this equation, D is the penetration depth of winter coldness into the ice.

We have prepared several criteria for zone boundaries: equations (5), (8), (9) and (10). We will confirm the validity of these equations in section 4., and propose three typical glacier types, consisting of possible glacier zones, in section 5-2.

4. ZONING OF THE YALA GLACIER

4-1. Estimation of surface balance and infiltration water

Annual surface balance, $b_a(s)$, and annual amount of infiltration water, Q_a , on the Yala Glacier were estimated from climatic elements (temperature and precipitation) on this glacier. The surface balance, $b(s)$, is the sum of surface accumulation (solid precipitation) and surface ablation, $a(s)$:

$$b(s) = \gamma P + a(s) \quad (11)$$

where γ is the probability of solid precipitation ($0 < \gamma < 1$) and P is the amount of precipitation. (The symbol (s) denotes the surface mass-balance term). Ageta and Higuchi (1984) described γ and $a(s)$ as the functions of semi-monthly mean air temperature (T_h °C), based on their field observations on a glacier in East Nepal, as follows:

$$\gamma_h = -0.24 T_h + 0.85 \quad (-0.6 < T_h < 3.5^\circ\text{C}) \quad (12)$$

$$a_h(s) = -1.5 (T_h + 3.0)^{3.2} \text{ (mmH}_2\text{O)} \quad (T_h > -3.0^\circ\text{C}) \quad (13)$$

where the subscript h denotes amount or value during a half of a month. The amount of infiltration water, Q , from the surface into the snow is the sum of the rain water and the ablation water (meltwater):

$$Q = (1-\gamma)P - a(s) \quad (14)$$

where $(1-\gamma)$ is the probability of liquid precipitation. From equations (11), (12), (13) and (14); we can calculate annual amounts of $b_a(s)$ and Q_a by the summation of each half month, if

we have climatic data, such as air temperature (T_h) and precipitation (P_h) on the glacier.

Air temperature and precipitation on the glacier were estimated from meteorological data observed at the meteorological station (BH) in Kyangchen (3920 m a.s.l., shown in Fig. 3-b). Figure 9 shows the smoothed seasonal variations of air temperature and monthly mean precipitation derived from our observations at BH from 1985 to 1989 (cf. Takahashi et al., 1987) and from observations of the Nepal Government at Timure from 1958 to 1970 (Ageta et al., 1984b). We assume the altitudinal lapse rate of air temperature to be 6.0 ($^{\circ}\text{C km}^{-1}$) from BH to the terminus of the glacier and 7.5 ($^{\circ}\text{C km}^{-1}$) on the glacier after studies by Takahashi et al. (1987) and by Ueno and Yamada (1990), respectively. We assumed that the amount of precipitation increases linearly with increasing altitude at the rate of 25.6 ($\% \text{ km}^{-1}$) from BH (3920m a.s.l.); this rate is based on field observations (Seko, 1987; Ueno and Yamada, 1990).

Figure 10 shows the altitudinal distributions of $b_a(s)$ and Q_a calculated on this glacier. The annual infiltration water, Q_a , (meltwater and rain water) decreases with increasing altitude, as a result of decreasing of summer air temperature. The annual surface balance, $b_a(s)$, is a residual part of annual precipitation ($b_a(s) = P_a - Q_a$), and increases with increasing altitude. The annual precipitation, P_a , is a nearly constant value (1300 - 1400 $\text{mmH}_2\text{O a}^{-1}$) on the glacier. As listed in Table II, the calculated amount, $b_a(s)$, roughly agrees with observed amount, b_n , during 1986-87.

4-2. Estimation of internal accumulation

We will solve the heat conduction equation, and estimate the freezing depth, D , and firn temperature during winter; we thereby evaluate the amount of internal accumulation, $c_a(i)$, by using equations (1) and (2). The one dimensional heat conduction equation including effect of latent heat is given by,

$$\rho c \frac{\partial \theta}{\partial t} + L \frac{\partial \omega}{\partial t} = \frac{\partial}{\partial z} \left[K \frac{\partial \theta}{\partial z} \right] \quad (15)$$

where t is time and K is thermal conductivity of firn. Firn temperature, θ , is zero when free water content of the firn, ω , is positive; and ω is zero when θ is negative. It has been confirmed that the amount of horizontal heat advection due to glacier flow and the amount of horizontal thermal diffusion are two and three orders of magnitude smaller than that of vertical thermal diffusion. We thus neglect the horizontal terms and treat this problem as a one dimensional problem for a first approximation. Since the above equation (15) becomes non-linear at the melting point, it is difficult to get an analytical solution. We therefore solve equation (15) numerically by means of the finite difference method (FDM). The method of numerical calculation is shown in Appendix II. The calculation is carried out with the following initial and boundary conditions.

We set the initial condition as the wet condition at the end of summer. The vertical distribution of firn density, ρ , is obtained by core analysis at each site. Firn temperature is set to the melting point, and volumetric free water content of the firn

is assumed to be 5 % of the pore volume; this is based on our measurements at Y9-a in September, 1987. In the superimposed-ice zone and ablation zone, we initially set ice temperature at -1°C (dry condition) and then change it to an appropriate value by the one year simulation as described below. Thermal conductivity, K ($\text{W m}^{-1} \text{K}^{-1}$), is estimated from the firn density by the following empirical equation (Murakami and Maeno, 1989):

$$K = \begin{cases} 0.049 \exp(4.75\rho) & \text{for } \rho < 0.65 \text{ (Mg m}^{-3}\text{)} \\ 0.172 \exp(2.80\rho) & \text{for } \rho \geq 0.65 \text{ (Mg m}^{-3}\text{)} \end{cases} \quad (16)$$

The surface boundary conditions, such as surface temperature and surface accumulation, are estimated from climatic data at Kyangchen (BH) as presented in the previous section (Fig. 9). We assume that the winter season is the period when the air temperature is lower than -3°C , since surface melting does not significantly occur in such temperature conditions (see Eq. (13); Ageta and Higuchi, 1984). As an example, the dotted line in Fig. 9 shows a -3°C line estimated at Y9 (5304 m a.s.l.). The winter season begins in October and ends in the middle of May. This is consistent with our observations: surface refreezing began from October in 1987 at Y9. We assume that surface temperature of the glacier is same as air temperature. We take into account the effect of thermal insulation due to winter snowfall. The thickness of the winter snowfall is estimated by $\Sigma P/\rho_w$; where ΣP is the cumulative precipitation from the beginning of winter and ρ_w is the mean density of the winter snowfall. We set ρ_w as 0.34 (Mg m^{-3}); this is based on pit work conducted at Y9 in April,

1986 by Motoyama (personal communication).

On the basis of the above initial and boundary conditions, we simulate the freezing depth, D , and the internal accumulation, $c_a(i)$, at each site on the Yala Glacier (5150 m, Y4, Y5, Y6, Y7, Y9, Y10, Y11, Y12 and 5500 m). The estimated values of $c_a(i)$ are shown in Fig. 10 and also in Table II with D .

As an example in the temperate infiltration zone, Fig. 11 shows a simulated result on the penetration process of winter coldness at Y9 (5304m a.s.l.). The maximum penetration depth, D , reaches the depth of 6 m on May 16, the end of the winter season. Using this freezing depth and the vertical distribution of firn temperature at May 16, we estimate the maximum value of internal accumulation, $c_a(i)^*$, as 171 ($\text{mmH}_2\text{O a}^{-1}$) from equation (4). Since the infiltration water, Q_a , is 797 ($\text{mmH}_2\text{O a}^{-1}$) at this site (see Table II), this site satisfies the temperate condition ($Q_a > c_a(i)^*$: Eq. (5)), and firn temperature can be at the melting point throughout by late summer. Thus, $c_a(i) = c_a(i)^*$. Figure 10 shows that all observation sites in this zone (Y9-Y12) satisfy the temperate condition; this agrees with our observations. While, it appears that the area above the altitude of 5480 m a.s.l. is the cold infiltration zone; the internal accumulation is restricted by the amount of infiltration water ($c_a(i) = Q_a < c_a(i)^*$).

As an example in the superimposed-ice zone, Fig. 12-a shows a simulated result on the penetration process of winter coldness at Y7 (5269 m a.s.l.). The winter coldness intrudes into glacier body to the depth of 10 m on May 15 as a result of high thermal

conductivity of ice and of no free water content in the ice; thus $D=10$ m. In this zone, a considerable amount of infiltration water is supplied from the surface during summer; this water is, however, shut out at the upper surface of the ice mass because of its impermeability to water. Thus, ice temperature from below the surface is warmed up only by the heat conduction. We simulate this process by assuming the temperature of the ice surface to be at 0°C during the summer season (May to September). Fig. 12-b shows the simulated result that ice temperature nearly returns to the initial temperature (-1°C) by October 1. We thereby confirm consistency of our simulation, and consider this temperature (-1°C) to be the temperature, θ_i , at the isothermal depth (10 m depth). The amount of internal accumulation, $c_a(i)$, is calculated as 190 ($\text{mmH}_2\text{O a}^{-1}$) by equation (3). At lower sites (Y6, Y5, Y4, 5150 m and 5100 m), we estimate the temperature, θ_i , as -2°C (Table II). The estimated temperature (-1 to -2°C) at the isothermal depth is consistent with the observed temperature (-1°C) at Y4 (Fig. 4; Watanabe et al., 1984).

It appears that the amount of internal accumulation is approximately constant (140 to 200 $\text{mmH}_2\text{O a}^{-1}$) in the area where the temperate condition is satisfied (<5480 m a.s.l.). The isothermal temperature, however, varies critically at the stratigraphic boundary.

4-3. Zoning of the Yala Glacier

Altitudinal distribution of $c_a(i)$, Q_a and $b_a(s)$ estimated on the Yala Glacier are shown in Fig. 10. From this figure, we can

determine the zone boundaries as follows:

(1) $Q_a = c_a(i)^*$ (Eq. (5)) at the altitude of 5480 m a.s.l.: the boundary between cold and temperate infiltration zone.

(2) $b_a(s) = \alpha c_a(i)$ (Eq. (8) with $\alpha = 1.2$) at the altitude of 5250 m: the upper boundary of the superimposed-ice zone.

(3) $b_a(s) + c_a(i) = 0$ (Eq. (9)) at the altitude of 5190 m: the equilibrium line.

The dry snow zone (there is no surface melting) can be estimated by $Q_a = 0$. We estimate the zone boundary between the dry snow zone and the cold infiltration at an altitude of 5900 m a.s.l. Hence, in the case of the Yala Glacier, the dry snow zone is absent. We estimate the boundary between the cold ablation zone and the temperate ablation zone (Eq. (10)) at an altitude of 4700 m a.s.l. Hence, the whole of the ablation area of this glacier belongs to the cold ablation zone where ice temperature at the isothermal depth (10 m) is negative (-1 to -2°C).

We, therefore, divide the Yala Glacier into the following four zones by the estimated amounts (Q_a , $c_a(i)^*$ and $b_a(s)$):

(1) "cold infiltration zone" (5480-5600 m):

$$Q_a < c_a(i)^* \text{ and } b_a(s) > \alpha c_a(i), (c_a(i) = Q_a)$$

(2) "temperate infiltration zone" (5250-5480 m):

$$Q_a > c_a(i)^* \text{ and } b_a(s) > \alpha c_a(i), (c_a(i) = c_a(i)^*)$$

(3) "superimposed-ice zone" (5190-5250 m):

$$-c_a(i) < b_a(s) < \alpha c_a(i)$$

(4) "cold ablation zone" (5100-5190 m):

$$b_a(s) < -c_a(i)$$

The above estimation agrees well with our observations

carried out in the late summer of 1987: (1) the temperate infiltration zone extends from 5270 m (above Y7) to at least 5458 m (Y12); (2) the superimposed-ice zone extends from lower than the snow line of 5210 m to 5270 m; (3) the cold ablation zone is located in the area below the snow line of 5210 m. We have confirmed validity of our equations (5) and (8). By using these equations, we can predict internal stratigraphy and temperature conditions in any given glacier in the world, if we can estimate the amounts (Q_a , $c_a(i)^*$ and $b_a(s)$) on the glacier.

5. GENERAL CLASSIFICATION OF GLACIERS IN THE WORLD

5-1. Generalized glacier zone model

Figure 13 shows an idealized glacier which consists of six different thermal zones. Occurrence and extent of each zone is determined by the following relational equations among infiltration water (Q_a), internal accumulation ($c_a(i)^*$ or $c_a(i)$) and surface balance ($b_a(s)$) as follows:

- (1) dry snow zone: $Q_a = 0$
- (2) cold infiltration zone: $Q_a < c_a(i)^*$ and $b_a(s) > \alpha Q_a$
- (3) temperate infiltration zone: $Q_a > c_a(i)^*$ and $b_a(s) > \alpha c_a(i)^*$
- (4) superimposed-ice zone: $-c_a(i) < b_a(s) < \alpha c_a(i)$
- (5) cold ablation zone: $-D\rho_i - c_a(i) < b_a(s) < -c_a(i)$
- (6) temperate ablation zone: $b_a(s) < -D\rho_i - c_a(i)$

where $\alpha = \rho_s / (\rho_i - \rho_s)$ and D is the penetration depth of winter coldness.

The dash-dotted line in Fig. 13 represents the isotherm of the melting point at the end of summer. The temperature at the isothermal depth (10 m depth) is cold at (1), (2), (4) and (5), whereas it is temperate at (3) and (6).

Every glacier does not always contain all zones; some zone is often absent. In the following sections, we will discuss the possible combinations of these zones under several specific climatic conditions.

5-2. Temperate, cold and inversion type glacier

We will propose here three typical glacier types: (a) temperate type, (b) cold type, and (c) inversion type. The type (a)

and (b) have been called temperate and sub-polar, respectively.

The temperate type glacier is characterized by the absence of superimposed-ice and cold ablation zones. Hence, it consists of a temperate ablation zone and a temperate infiltration zone: (6)+(3)+. The plus sign means that there can be a cold infiltration zone and a dry snow zone in its upper part where Q_a is less, if the glacier is largely extended. Thus we call this glacier as a temperate type instead of "temperate". The condition for absence of superimposed-ice zone ($-c_a(i) < b_a(s) < \alpha c_a(i)$) and cold ablation zone ($-D\rho_i - c_a(i) < b_a(s) < -c_a(i)$) is given by,

$$c_a(i) = D = 0 \quad (17)$$

This is the necessary condition for a temperate type glacier. As confirmed below, only a few glaciers satisfy this condition. We thus believe many glaciers, which have been classified as temperate glaciers, should have a "cold" ice zone near the equilibrium line when air temperature on the glacier is cold in winter.

The difference between an inversion type glacier and a cold type glacier is whether it has a temperate infiltration zone or not. The inversion type glacier consists of a cold ablation zone, superimposed-ice zone and temperate infiltration zone: +(5)+(4)+(3)+. On the other hand, the cold type glacier consists of a cold ablation zone, superimposed-ice zone and cold infiltration zone: +(5)+(4)+(2)+. The condition for existence of the temperate infiltration zone ($Q_a > c_a(i)^*$ and $b_a(s) > \alpha c_a(i)^*$) can be expressed as the following simple equation, because $Q_a + b_a(s) = P_a$ (annual precipitation):

$$P_a > (1+\alpha)c_a(i)^* \quad (18)$$

This is the necessary condition for occurrence of the inversion type glacier. The above equation (18) shows that if annual precipitation is 2-2.5 times larger than the amount of maximum internal accumulation, the temperate infiltration zone can appear in the accumulation area of the glacier. On the contrary, if annual precipitation is less than this amount, then the temperate zone will vanish, and the superimposed-zone will be directly converted into the cold infiltration zone with increasing altitude.

By using equations (17) and (18), we can classify any glacier in the world into one of three typical glacier types, if we can estimate annual precipitation and internal accumulation on each glacier.

5-3. General classification

For convenience of general use, we will replace the maximum amount of internal accumulation, $c_a(i)^*$, by freezing index (i.e., cumulative negative daily mean temperature during winter). For this purpose, we first estimate $c_a(i)^*$ with various surface boundary condition (air temperature and precipitation). The freezing index, FI ($^{\circ}\text{C day}$), is calculated from the annual temperature variation. We thereby show a way to estimate $c_a(i)^*$ by freezing index and winter precipitation. Finally, we produce a diagram of freezing index versus annual precipitation by which glacier can be classified into one of three typical types: tem-

perate type, cold type and inversion type.

We estimate the amount of maximum internal accumulation, $c_a(i)^*$, (Eq. (4)) by numerical calculation of equation (15) as described in the section 4-2. Here we assume a sin curve for seasonal temperature variations on a glacier as:

$$T(t) = A \sin (2\pi t/t_a) + T_a \quad (20)$$

where A is a amplitude, T_a is annual mean air temperature and t_a is 365 (days). Let us assume that the winter season is the period when the air temperature is lower than -3°C , as assumed in the section 4-2. We set firn density to a linear distribution from 0.45 (Mg m^{-3}) at the surface to 0.80 at 10 m depth; this is similar to that at Y9 on the Yala Glacier. We assume constant snowfall during winter; the total winter precipitation is P_w . Other parameters are the same as those assumed in section 4-2. Numerical calculation is carried out with various variations of air temperature ($-16 < T_a < 0$ and $2 < A < 20$) and various amounts of winter precipitation ($0 < P_w < 4000 \text{ mmH}_2\text{O}$).

On the other hand, the freezing index, FI ($^\circ\text{C day}$), is given by integration of equation (20) as,

$$FI = \frac{t_a}{\pi} \{ \sqrt{A^2 - (-3 - T_a)^2} - T_a \sin^{-1} (-3 - T_a) / A - \pi T_a / 2 \} \quad (21)$$

We estimate FI by T_a and A with this equation.

Figure 14 shows the relation between $c_a(i)^*$ calculated with heat conduction equation and FI calculated by Eq. (21). The maximum annual internal accumulation, $c_a(i)^*$, increases with

increasing freezing index, FI, and decreases with increasing winter precipitation, P_w . By using this figure, we can estimate $c_a(i)^*$ from freezing index, FI, and winter precipitation, P_w .

Figure 15 is the diagram showing three glacier types and climatic conditions (freezing index and annual precipitation). The boundary condition between the inversion type glacier and the cold type glacier (Eq (18) with $\alpha=1.2$) is given in this figure. For practical use, condition for the temperate type glacier is also given in this figure as $D < 3$ (m) and $c_a(i)^* < 80$ ($\text{mmH}_2\text{O a}^{-1}$) instead of equation (17). The solid circles represent the inversion type glaciers listed in Table I, and open circles represent cold type glaciers without a temperate infiltration zone listed in Table III. FI and P_a are estimated at the equilibrium line or the snow line on each glacier. The actual glaciers agree fairly well with the theoretically predicted lines. Thus we conclude that (1) the inversion type glacier can occur when freezing index is more than 2000 ($^{\circ}\text{C day}$) and annual precipitation exceeds 700 ($\text{mmH}_2\text{O a}^{-1}$) and (2) the cold type glacier can be occur when precipitation is less than 700 ($\text{mmH}_2\text{O a}^{-1}$). This result explains the empirical result that cold type glacier (sub-polar glacier) has often been observed in continental climate regions where annual precipitation is little.

6. DISCUSSION

6-1. Effect of zone boundary on glacier flow

Temperature condition at the base of glacier has a strong effect on glacier flow. For instance, lower part of the Yala Glacier (Fig. 6) is frozen to the bed rock, and thus there seems to be no basal sliding. On the other hand, its upper part is completely at the melting point, there should be basal sliding. Hence, the glacier movement is restricted and reduced at the transitional zone between melting and freezing. In this section, we will investigate a flow pattern and a stress field around such a transitional zone.

The basic equations for ice deformation are the flow law of ice and the continuity equation of incompressible mass. The flow law is

$$\dot{\epsilon} = E \tau^n \quad (22)$$

where $\dot{\epsilon}$ is effective strain rate, E is the flow law parameter, τ is the effective shear stress and n is the index about 3. The two dimensional (x, z) continuity equation of mass is given by,

$$\frac{\partial u}{\partial x} + \frac{\partial w}{\partial z} = 0 \quad (23)$$

where (u, w) is longitudinal (x) and vertical (z) components of the flow velocity. For a rough estimation, we assume, in a transitional zone, that basal sliding velocity decreases with x at a constant rate: $du_b/dx = -r$, and that stress components and strain-rate components are independent of x . This is plausible for a long parallel-sided slab of constant slope. On the above

assumptions, we can solve equations (22) and (23) by a method given by Nye (1957). The method and appropriate boundary conditions for the case of Yala Glacier are shown in Appendix III.

Figure 16 shows calculated result of flow velocity and normal-stress components (σ_x , σ_z) in the transitional zone of the Yala Glacier. It is shown that the transitional zone is a compression zone where compressive stress difference ($\sigma_x - \sigma_z$) is from 40 to 120 (kPa), and upward movement of ice occurs as the result of compression; the velocity is 2.2 (m a^{-1}) at the surface. Ageta et al. (1984a) observed a vertical component of velocity of 1.2 to 1.8 (m a^{-1}) against snow surface (i.e., the emergence velocity) in the superimposed-ice zone and in the ablation zone on the Yala glacier in 1982. If the glacier bed is approximately parallel to the glacier surface, we can consider that this emergence velocity is caused by the compression of ice at the transitional zone. A similar phenomenon was observed by Collins (1972) on Rusty Glacier in Yukon Territory, Canada. He concluded that the lower part of the Rusty Glacier acts as ice "dam" against glacier movement. Later on, it appears that basal temperature of this glacier shows temperature inversion (Clarke and Goodman, 1975). Further investigation is necessary to confirm the upward movement of ice at the compression zone at the melting to freezing transition.

On the contrary, the boundary of freezing to melting transition, e.g., the transitional zone between cold infiltration zone and temperate infiltration zone, is an extension zone. In this zone, downward movement of ice (i.e., submergence flow) is expected. If the tensile stress is high, a crevasse can be formed

at this transitional zone as discussed by Lliboutry et al. (1976).

Figure 17 shows schematic flow lines drawn on the idealized glacier. It should be noted that glacier flow is affected by the temperature condition in a glacier as well as by the bed rock topography and roughness of the bed.

6-2. Instability of the inversion type glacier

The inversion type glacier is in a potentially unstable condition, because the upper mobile temperate snow and ice is stopped by the lower cold ice "dam" which is frozen to the bed rock (see e.g. Fig. 6). If the "dam" happens to be broken for some reasons, a rapid advance will occur with a positive feedback system, e.g., creep heat production, and cracking and infiltration of water into the ice.

Moreover, the cold impermeable ice seems to dam up water from the upper temperate infiltration zone. Figure 18 shows the "water storage system" occurring in a ice cap; this is rewritten from figure 2 after Schytt (1969). In the temperate infiltration zone, considerable amount of water ($Q_a - c_a(i)^*$) infiltrates into the deeper firn layer. The temperate ice is known to be slight permeable. Thus the temperate ice can be saturated with water. Indeed, we observed water spouting out from the ice during drilling observations at Y9-a and Y11 on the Yala Glacier. If the level of the water rises higher, this water will brake the lower ice "dam" and cause a glacier surge with a lot of water discharge, like "jokulhlaup". Further investigation is necessary to

clarify the role of the water storage system in glacier surge.

In the Himalayan regions, there are many thick debris covered glaciers. This debris covered ice is considered to be a relic ice which had advanced in the Little Ice Age as described in section 2-1. The existence of such ice masses suggests that the stability was broken in that age. For instance, if we consider that the mean air temperature is gradually lowered 2°C , the zone boundary at the altitude of 5270 m on the Yala Glacier will go downward about 250 m in altitude in accordance with equation (8). This means that the cold ice "dam" will be buried by snow and will become "temperate" throughout; it may produce a rapid and great advance of the glacier. Here, we would like to point out that the fluctuation of glacier is greatly affected by changing of thermal condition (zonal condition) in a glacier as well as by changing of mass balance on a glacier.

Again, we would like to point out that all glaciers with temperature inversion are in a potentially unstable condition. According to Post (1969), many surge type glaciers are located in a transitional area from maritime climate to continental climate. Such an area might be cold in winter ($\text{FI} > 2000^{\circ}\text{C day}$) and there will be considerable precipitation ($\text{P}_a > 700 \text{ mmH}_2\text{O}$). Thus we believe that the inversion type glacier can be a surge type glacier. (Some surge type glaciers may not be the inversion type, of course.) Indeed, the ice cap of Vestfonna and Black Rapid Glacier (Table I) are well-known surging glaciers. Further investigation will be very useful to confirm the relationship of the inversion type glacier to the surge type glacier throughout the world.

7. CONCLUDING REMARKS

We have stated that thermal regime and stratigraphic conditions of a glacier are determined by three amounts of water, i.e., annual infiltration water: Q_a , annual internal accumulation: $c_a(i)$ and annual surface balance: $b_a(s)$. A glacier can be divided into several zones with different thermal conditions according to the relation among Q_a , $c_a(i)$ and $b_a(s)$.

In this study, the most important findings are summarized as follows:

- (1) The inversion type glaciers, which are in disagreement with previous classification such as temperate or sub-polar glaciers, are widely distributed in the world.
- (2) This glacier has a temperate zone (temperature is at the melting point throughout) in the accumulation area and a cold zone (temperature is negative) in the ablation area.
- (3) Such glacier can be found in the regions where winter is cold (the freezing index exceeds 2000°C day) and annual precipitation is more than 700 (mmH₂O).
- (4) Such glacier is in a potentially unstable condition, because the upper mobile temperate ice is dammed up by the lower cold ice frozen to the bed rock. This instability can produce a rapid advance of the glacier, i.e., the glacier surge.

ACKNOWLEDGMENTS

The author would like to express his particular gratitude to Prof. G. Wakahama and Dr. T. Yamada of the Institute of Low Temperature Science (I.L.T.S.), Hokkaido University, for their encouragement and useful suggestions throughout the study. He also wishes to express to gratitude to Prof. K. Nakao of the Department of Geophysics, Faculty of Science, Hokkaido University, Prof. D. Kobayashi and Dr. R. Naruse of I.L.T.S., Dr. M. Nakawo of Nagaoka Institute of Snow and Ice Studies, Mr. T. Hasemi of Snow and Ice Research Inc., and Dr. H. Motoyama of National Institute of Polar Research for their helpful discussions in preparing this paper. He is also grateful to all members of Glaciological Expedition of Nepal Himalaya 1987-88 (GEN 87), especially to Mr. S. Murakami of Kyosera Inc. for numerous discussions in the field.

Appendix I

List of symbols

| | |
|---------------------|---|
| a(s) | Surface ablation |
| a _h (s) | Surface ablation during half month |
| A | Amplitude of seasonal air temperature variation |
| b(s) | Surface balance |
| b _a (s) | Annual surface balance |
| b _n | Net balance during 1986-87 |
| c _w (i) | Internal accumulation during winter |
| c _a (i) | Internal accumulation during summer |
| c _a (i) | Annual internal accumulation |
| c _a (i)* | Maximum annual internal accumulation |
| d | Thickness of annual layer |
| D | Freezing depth or penetration depth of winter coldness |
| E | Flow law parameter ($5.3 \times 10^{-24} \text{ s}^{-1} \text{ Pa}^{-3}$) |
| FI | Freezing index |
| K | Thermal conductivity |
| L | Latent heat of fusion of ice |
| n | Flow law index (3) |
| P | Precipitation |
| P _h | Precipitation during half month |
| P _w | Precipitation during winter |
| P _a | Annual precipitation |
| ΣP | Cumulative precipitation during winter |
| Q | Infiltration water |
| Q _a | Annual infiltration water |
| r | Decreasing rate of basal sliding velocity |

| | |
|------------------|--|
| t | Time |
| t _a | 365 days |
| T | Air temperature |
| T _h | Half month mean air temperature |
| T _a | Annual mean air temperature |
| u | Longitudinal component of flow velocity |
| u _b | Basal sliding velocity |
| w | Vertical component of flow velocity |
| x | Longitudinal axis |
| z | Vertical axis |
| α | $\rho_s / (\rho_i - \rho_s)$, a parameter for ice formation |
| $\dot{\epsilon}$ | Effective strain rate |
| γ | Probability of solid precipitation |
| γ_h | Probability of solid precipitation during half month |
| σ_x | Longitudinal component of normal-stress |
| σ_z | Vertical component of normal-stress |
| ρ | Density of snow and firn |
| ρ_s | Density of initial snow at the surface |
| ρ_i | Ice transition density (0.83 Mg m ⁻³) |
| ρ_w | Density of winter snowfall |
| $\Delta\rho$ | Density increase of firn due to freezing |
| τ | Effective shear stress |
| ω | Free water content per unit volume |
| θ | Firn temperature |
| θ_e | Firn temperature at end of summer |
| θ_b | Firn temperature at beginning of summer |

Appendix II

Method of numerical calculation

In order to solve equation (15), we use apparent amount of heat content per unit volume, f , as (Carslaw and Jaeger, 1959; p. 477):

$$f = \begin{cases} \rho c \theta & \text{for } \theta < 0^\circ\text{C} \\ L\omega & \text{for } \theta = 0^\circ\text{C} \end{cases} \quad (\text{A1})$$

The explicit scheme of finite difference approximation for the equation (15) is, then, given by,

$$f(i,j) = f(i,j-1) + \frac{\Delta t}{\Delta z^2} K(i) \{ \theta(i-1,j-1) + \theta(i+1,j-1) - 2\theta(i,j-1) \} \quad (\text{A2})$$

$$\begin{cases} \text{if } f(i,j) < 0 \text{ then } \theta(i,j) = f(i,j)/\rho(i)c \text{ and } \omega(i,j) = 0 \\ \text{if } f(i,j) > 0 \text{ then } \theta(i,j) = 0 \text{ and } \omega(i,j) = f(i,j)/L \end{cases} \quad (\text{A3})$$

where $f(i,j)$ and $\theta(i,j)$ are the heat content and temperature at depth $z=i\Delta z$ and at time $t=j\Delta t$, respectively.

To achieve a stable solution, we must set the time step (Δt) and the depth segment (Δz) as:

$$\frac{K_{\max} \Delta t}{\rho_{\min} c \Delta z^2} < 0.5 \quad (\text{A4})$$

We set $\Delta t=1$ (hour) and $\Delta z=10$ (cm), and calculate equations (A2) and (A3) by a personal computer.

Appendix III

Analysis of glacier flow in the transitional zone

This analysis follows that of Nye (1957). We have assumed that all stress components are independent of x and y . Then the equations of static equilibrium expressing the balance between the forces applied to a small cube with sides parallel to the coordinate axes are

$$\frac{\partial \tau_{xz}}{\partial z} = -\rho g \sin \beta \quad (\text{A5})$$

$$\frac{\partial \sigma_z}{\partial z} = -\rho g \cos \beta \quad (\text{A6})$$

where τ_{xz} is shear-stress component, σ_z is normal-stress component and β is the slope of the slab. We can easily integrate equations (A5) and (A6) with appropriate boundary conditions:

$$\tau_{xz} = -\rho g z \sin \beta \quad (\text{A7})$$

$$\sigma_z = -p - \rho g z \cos \beta \quad (\text{A8})$$

where p is the atmospheric pressure.

The strain rate components can be given by the flow law equation (Nye, 1957):

$$\frac{\partial u}{\partial x} = E \tau^{n-1} \sigma_x' \quad (\text{A9})$$

$$\frac{\partial u}{\partial z} = 2E \tau^{n-1} \tau_{xz} \quad (\text{A10})$$

By substituting (A7) into (A10) and integrating it with z from z to h (bottom), we get the longitudinal velocity component:

$$u = u_b + 2E\rho g \sin \beta \int_z^h \tau^{n-1} z \, dz$$

$$u_b = u_0 - rx \tag{A11}$$

where u_0 is the sliding velocity at $x=0$, and r is a constant decreasing rate of the sliding velocity. In order to satisfy the continuity equation (23), the vertical velocity component must be

$$w = -r(h-z) \tag{A12}$$

The negative sign denotes upward movement.

By the definition, the effective shear stress and stress-deviator are

$$\tau^2 = \sigma_x'^2 + \tau_{xz}^2 \tag{A13}$$

and

$$2\sigma_x' = (\sigma_x - \sigma_z) \tag{A14}$$

From equations (A7), (A9) with (A11), and (A13), we can calculate τ as the function of z . Then, we can integrate the second term in the equation (A11) numerically. We thereby evaluate the flow velocity (u , w) and normal stress components (σ_x , σ_z) in the transitional zone of the Yala Glacier.

The boundary conditions are summarized as follows:

- (1) Ice thickness is 50 m in the melting zone and 65 m in the freezing zone.
- (2) The length of the transitional zone is 300 m.
- (2) The slope angle is a constant value of 15° .

(3) Surface flow velocity is $20 \text{ (m a}^{-1}\text{)}$ in the melting zone and $14 \text{ (m a}^{-1}\text{)}$ in the freezing zone. Then the sliding velocity at the bottom is estimated to be $14 \text{ (m a}^{-1}\text{)}$.

REFERENCES

- Ahlmann, H. W., 1935: Contribution to the physics of glaciers. *Geographical J.*, 86, 97-113.
- Ageta, Y. and K. Higuchi, 1984: Estimation of mass balance components of a summer-accumulation type glacier in the Nepal Himalaya. *Geogr. Ann., Ser. A*, 66(3), 249-255.
- Ageta, Y., H. Iida and K. Higuchi, 1984a: Glaciological studies on Yala Glacier in Langtang Himal. Publication No.2, Data Center for Glacier Research, Japanese Society of Snow and Ice, 41-47.
- Ageta, Y., T. Yamada and K.B. Thapa, 1984b: Climate of Langtang Valley. Publication No.2, Data Center for Glacier Research, Japanese Society of Snow and Ice, 113-115.
- Benson, C.S., 1959: Physical investigations on the snow and firn of northwest Greenland 1952, 1953 and 1954. US Snow Ice and Permafrost Research Establishment. Research Report 26.
- Carslaw, H.S. and J.C., Jaeger, 1959: Conduction of heat in solids. Second edition. Oxford Univ. Press (Clarendon); London/New York.
- Cary, P.W., G.K.C. Clarke and W.R. Peltier, 1979: A creep instability analysis of the Antarctic and Greenland ice sheets. *Can. J. Earth Sci.*, 16, 182-188.
- Casassa, G., 1989: Velocity, heat budget and mass balance at Anvers Island Ice Cap, Antarctic Peninsula. *Antarctic Record*, 33(3), 341-352.
- Clarke, G.K.C., 1976: Thermal regulation of glacier surging. *J. Glaciol.*, 16(74), 231-250.

- Clarke, G.K.C., R.H. Goodman, 1975: Radio echo soundings and ice-temperature measurements in a surge-type glacier. *J. Glaciol.*, 14(70), 71-78.
- Collins, S.G., 1972: Survey of the Rusty Glacier area, Yukon Territory, Canada, 1967-70. *J. Glaciol.*, 11(62), 235-253.
- Fujii, Y. and K. Higuchi, 1977: Statistical analyses of the forms of the glaciers in the Khumbu Himal. *Seppyo Special Issue*, 39, 7-14.
- Fushimi, H., 1978: Glaciations in the Khumbu Himal (2). *Seppyo Special Issue*, 40, 71-77.
- Haeberli, W., 1976: Eistemperaturen in den Alpen. *Z. Gletscherkd. Glazialgeol.*, 11, 203-220.
- Harrison, W.D., L.R. Mayo and D.C. Trabant, 1975: Temperature measurements on Black Rapids Glacier, Alaska, 1973. in "Climate of the Arctic" (G. Weller and S.A. Bowing eds.), Geophysical Institute, University of Alaska, 350-352.
- Iida, H., O. Watanabe, M. Takikawa, 1984: First results from Himalayan Glacier boring project in 1981-1982; Part II. Studies on internal structure and transformation process from snow to ice of Yala Glacier, Langtang Himal, Nepal. Publication No.2, Data Center for Glacier Research, Japanese Society of Snow and Ice, 25-33.
- Jare Data Reports, 1983-1987, No 86, 101, 107, 120, 130., National Institute of Polar Research, Tokyo.
- Lliboutry, L., M. Briat, M. Creseveur and M. Pourchet, 1976: 15 m deep temperatures in the glaciers of Mont Blanc (French Alps). *J. Glaciol.*, 16, 197-203.

- Loewe, F., 1966: The temperature of the Sukkertoppen ice cap. *J. Glaciol.*, 6, 179.
- Motoyama, H., Personal communication (1988).
- Müller, F., 1962: Zonation in the accumulation area of the glaciers of Axel Heiberg Island, NWT, Canada. *J. Glaciol.*, 4(33), 302-311.
- Müller, F., 1976: On the thermal regime of a high-arctic valley glacier. *J. Glaciol.*, 16(74), 119-133.
- Murakami, S. and N. Maeno, 1989: Thermal conductivity of snow and snow/metal mixtures. *Low Temperature Science, Ser. A*, 48, (With English summary) 13-25.
- Murakami, S., H. Ozawa and T. Yamada, 1989: Permeability coefficient of water in snow and firn at the accumulation area of Yala Glacier, Nepal Himalaya. *Bulletin of Glacier Research*, 7, 203-208.
- Nye, J.F., 1957: The distribution of stress and velocity in glaciers and ice-sheets. *Proc. R. Soc. London, Ser. A*, 239, 113-133.
- Ohata, T., S. Takahashi and K. Xiangcheng, 1989: Meteorological conditions of the West Kunlun Mountains in the summer of 1987. *Bulletin of Glacier Research*, 7, 67-76.
- Ohata, T., K. Xiangcheng and S. Takahashi, 1990: Full year surface meteorological data at northwestern Tibetan Plateau using an automatic observation system. *Bulletin of Glacier Research*, 8, 73-85.
- Ohmura, A., 1987: New temperature distribution maps for Greenland. *Z. Gletscherkd. Glazialgeol.*, 23, 1-45.

- Palosuo, E., 1987: Ice layers and superimposition of ice on the summit and slope of Vestfonna, Svalbard. *Geogr. Ann., Ser. A*, 69(2), 289-296.
- Paterson, W.S.B., 1972: Temperature distribution in the upper layers of the ablation area of Athabasca Glacier, Alberta, Canada. *J. Glaciol.*, 11(61), 31-41.
- Paterson, W.S.B., 1981: *The physics of glaciers*. Second edition. Pergamon Press.
- Post, A, 1969: Distribution of surging glaciers in western North America, *J. Glaciol.*, 8(53), 229-240.
- Schytt, V., 1968: Notes on glaciological activities in Kevne-kaise, Sweden during 1966 and 1967. *Geogr. Ann. Ser. A*, 50(2), 111-120.
- Schytt, V., 1969: Some comments on glacier surges in eastern Svalbard. *Can. J. Earth Sci.*, 6, 867-873.
- Seko, K., 1987: Seasonal variation of altitudinal dependence of precipitation in Langtang Valley, Nepal Himalayas. *Bulletin of Glacier Research*. 5, 41-47.
- Shiraiwa, T. and T. Watanabe, Late quartanally glacier fluctuations in the Langtang Valley, Nepal Himalaya, reconstructed by relative dating methods. (submitted to *Arctic and Alpine Res.*)
- Shumskii, P.A., 1964: *Principles of structural glaciology*. (Translated from the Russian by David Kraus) New York, Dover Publications.
- Tanaka Y., Y. Ageta and K. Higuchi, 1980: Ice temperature near the surface of Glacier AX010 in Shorong Himal, East Nepal, *Seppyu Special Issue*, 41, 55-61.

- Takahashi, S., H. Motoyama, K. Kawashima, Y. Morinaga, K. Seko, H. Iida, H. Kubota and N.R. Turadahr, 1987: Meteorological features in Langtang Valley, Nepal Himalayas, 1985-1986. *Bulletin of Glacier Research*, 5, 35-40.
- Trabant, D.C., W.D. Harrison and C. Benson, 1975: Thermal regime of McCall Glacier, Brooks Range, northern Alaska. in "Climate of the Arctic" (G. Weller and S.A. Bowling eds.), Geophysical Institute, University of Alaska, 347-349.
- Trabant, D.C. and L.R. Mayo, 1985: Estimation of effects of internal accumulation on five glaciers in Alaska. *Ann. Glaciol.*, 6, 113-117.
- Ueno, K. and T. Yamada, 1990: Diurnal variation of precipitation in Langtang Valley, Nepal Himalayas. *Bulletin of Glacier Research*, 8, 93-101.
- Wakahama, G., 1968: The metamorphism of wet snow. *IAHS Publ.*, 79, 370-379.
- Wakahama, G., D. Kuroiwa, T. Hasemi and C. S. Benson, 1976: Field observations and experimental and theoretical studies on the superimposed ice of McCall Glacier, Alaska. *J. Glaciol.*, 74, 135-149.
- Watanabe, O., K. Ikegami, K. Kamiyama, S. Takenaka and T. Yamada, Unpublished, presented at Annual Meeting of Japanese Society of Snow and Ice, Oct. (1982).
- Watanabe, O., S. Takenaka, H. Iida, K. Kamiyama, K.B. Thapa and D.D. Mulmi, 1984: First results from Himalayan glacier boring project in 1981-1982; Part I. Stratigraphic analyses of full-depth cores from Yala Glacier, Langtang Himal, Nepal. Publica-

tion No.2, Data Center for Glacier Research, Japanese Society of Snow and Ice, 7-23.

Yamada, T., 1987: Glaciological characteristics revealed by 37.6-m deep core at the accumulation area of San Rafael Glacier, the Northern Patagonia Icefield. Bulletin of Glacier Research, 4, 59-67.

Yamada, T., 1989: An outline of Glaciological Expedition of Nepal: Langtang Himal Project 1987-88. Bulletin of Glacier Research, 7, 191-193.

Table I. Examples of the inversion type glaciers

| Area | Name | 10-m depth temperature ablation accumulation (°C) | Mean air temp. T _a (°C) | Annual range | | Annual Prec. P _a (mmH ₂ O·a ⁻¹) | Freezing Index FI (°C·day·a ⁻¹) | References |
|----------------|---------------|---|--|--------------|------------|---|---|------------|
| | | | | 2A (°C) | 2B (°C) | | | |
| Himalaya | Yala Gl. | -1 | -3.9~-7.7 | 14 | 1300 | 2000 | Watanabe et al., 1984 | |
| | AX010 | -2~-3 | -4.5~-7.0 | 13 | 1600 | 2100 | Tanaka et al., 1980 | |
| Alps | Mont Blanc | 0~-2 | 0~-16.7 | | | | Lliboutry et al., 1976 | |
| | Grubengletche | -1~-2 | 0 | | | | Haeberli, 1976 | |
| Scandinavia | Storglaciaren | -2~-3 | -4.7~-8.8 | 21 | 1500 | 2600 | Schytt, 1968 | |
| Canadian Rocky | Athabasca | -0.1~-1.5 | 0 | | | | Paterson, 1972 | |
| Alaska | Gulkana | -0.5 | 0 | | | | Trabant & Mayo, 1985 | |
| | Black Rapid | -0.6~-1.7 | 0 | | | | Harrison et al., 1975 | |
| Polar ice cap | McCall | -6~-10 | -8.9~-14.9 | 32 | 500 | 5200 | Trabant et al., 1975 | |
| | Vestfonna | -8~-10 | -8.8~-11.2 | 26 | 700 | 4180 | Schytt, 1969 | |
| | Sukkertoppen | (-) | -11.5~-14.9 | 25 | | 4160 | Loewe, 1966 | |
| | Anvers island | -0.8~-4.9 | -4.7~-10.6 | 12 | 4000 | 2840 | Casassa, 1989 | |

Table II. Altitudinal distribution of estimated and observed values on the Yala Glacier, Nepal Himalaya.
 $c_a(i)$: annual internal accumulation, $b_a(s)$: annual surface balance, b_n : net balance of 1986-87,
 Q_a : annual infiltration water, θ_i : temperature at isothermal depth.

| Coring site | Altitude (m a.s.l.) | Temp. T_a ($^{\circ}C$) | Depth D (m) | $c_a(i)$ | $b_a(s)$ ($mmH_2O \cdot a^{-1}$) | b_n | Q_a | θ_i ($^{\circ}C$) |
|-------------|---|-----------------------------|-------------|----------|------------------------------------|-------|-------|----------------------------|
| | | | | | | | | |
| - | 5100 | -4.0 | 10* | 168 | -1057 | - | 2372 | -2 |
| - | 5150 | -4.3 | 10* | 184 | -549 | - | 1881 | -2 |
| Y4 | 5200 | -4.7 | 10* | 193 | -116 | - | 1464 | -2 |
| - | 5210 (snow line) | | | | | | | |
| Y5 | 5224 | -4.9 | 10* | 206 | 69 | 30 | 1288 | -2 |
| Y6 | 5245 | -5.1 | 10* | 211 | 219 | 140 | 1145 | -2 |
| Y7 | 5269 | -5.2 | 10* | 190 | 378 | 510 | 994 | -1 |
| - | 5270 (upper limit of the superimposed ice zone) | | | | | | | |
| Y9 | 5304 | -5.5 | 6.0 | 171 | 587 | 810 | 797 | 0 |
| Y10 | 5349 | -5.8 | 4.4 | 141 | 523 | 1120 | 576 | 0 |
| Y11 | 5407 | -6.3 | 4.5 | 144 | 1070 | 1040 | 348 | 0 |
| Y12 | 5458 | -6.7 | 4.8 | 146 | 1245 | 2100 | 190 | 0 |
| - | 5500 | -7.0 | - | 101** | 1349 | - | 101 | (-) |
| - | 5600 | -7.7 | - | 26** | 1458 | - | 26 | (-) |

* The penetration depth of winter coldness

** This is identical with infiltration water (Q_a).

Table III. Examples of the cold type and temperate type glaciers

| Area | Name or Line | Mean air temp. T _a (°C) | Annual range 2A (°C) | Annual Prec. P _a (mmH ₂ O·a ⁻¹) | Freezing Index FI (°C·day·a ⁻¹) | References |
|----------------|----------------------|--|----------------------------|---|---|--------------------------|
| COLD TYPE | | | | | | |
| Kunlun, China | Chongce | -10.8~-14.5 | 23 | 300 | 4800 | Ohata et al., 1989, 1990 |
| Axel Heiberg | White | -18 | 34 | 200 | 6500 | Müller, 1962, 1976 |
| West Greenland | Jakobshavn-Centrale | -8.9~-30.4 | 28 | 400 | 6200 | Ohmura, 1987 |
| Antarctica | Syowa-Dome F | -9.6~-49.8 | 24 | 300 | 5100 | JARE, 1983-1987 |
| TEMPERATE TYPE | | | | | | |
| Patagonia | San Rafael-DS(1298m) | 7.6~-0.2 | 9 | 7500~10000 | 300 | Yamada, 1987 |

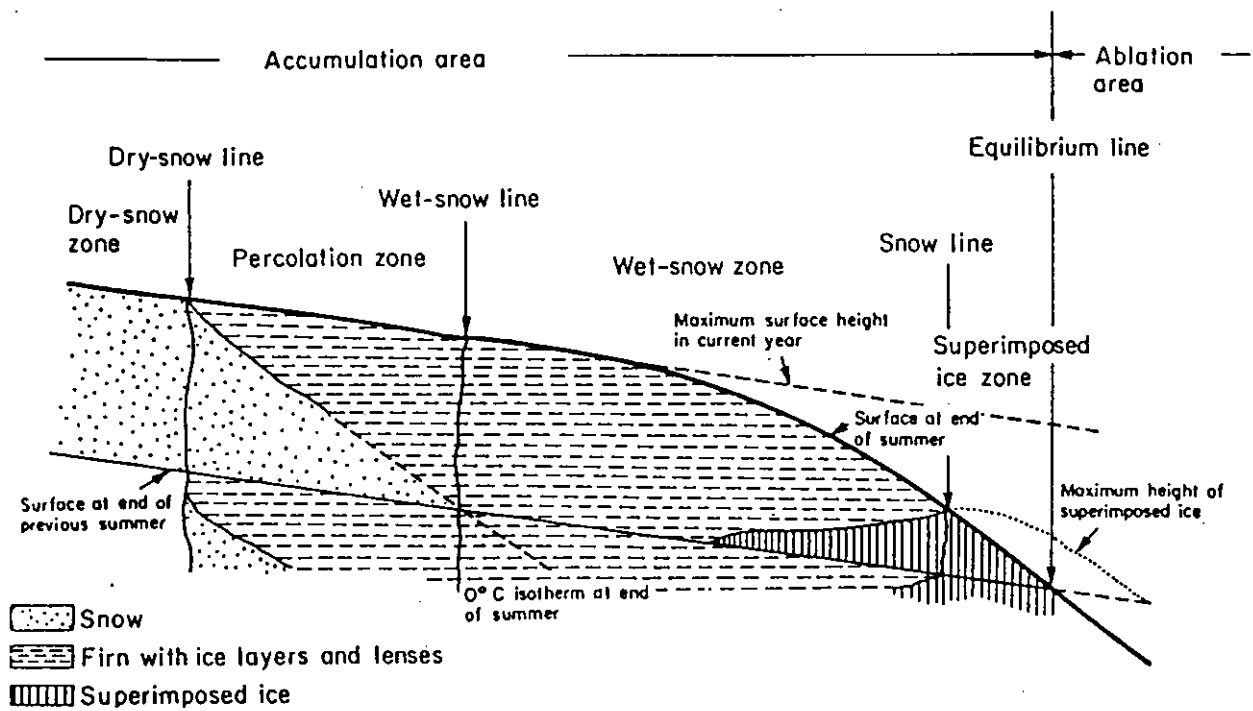


Fig. 1. Zones of accumulation area based on Benson (1959) and Müller (1962). After Paterson (1981).

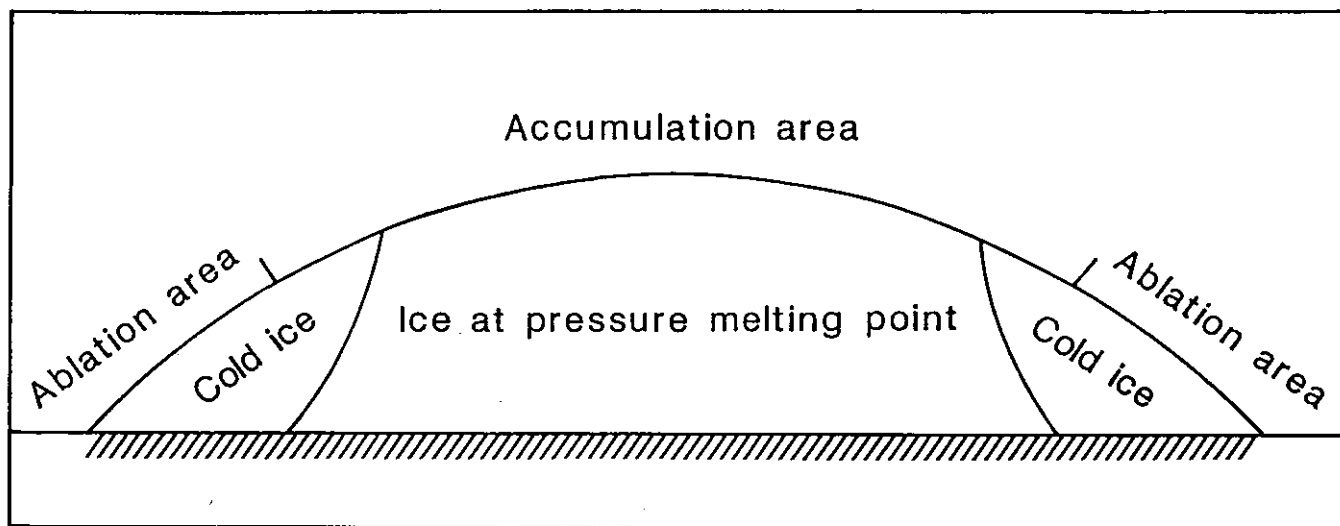


Fig. 2. Vertical section of an ice cap in eastern Svalbard.
After Schytt (1969).

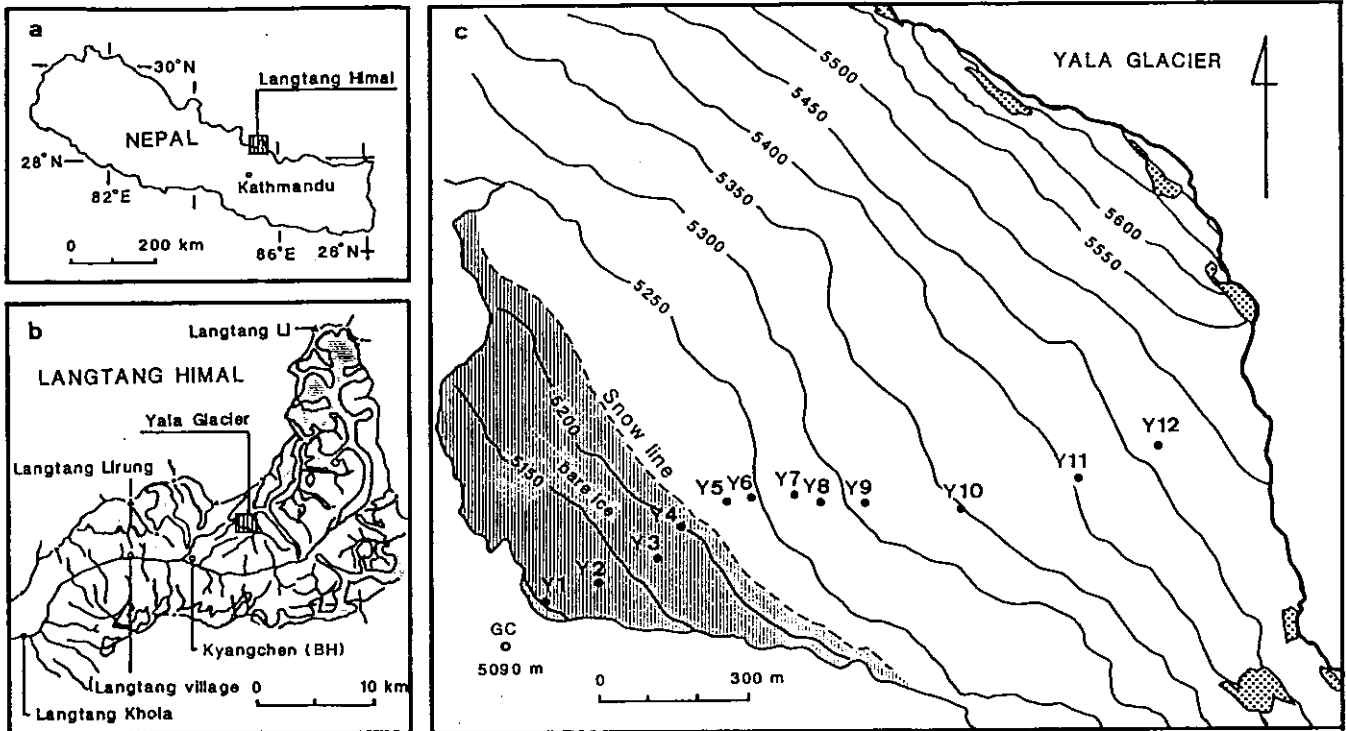


Fig. 3. Location and topography of the Yala Glacier in the Langtang Himal, Nepal Himalayas.

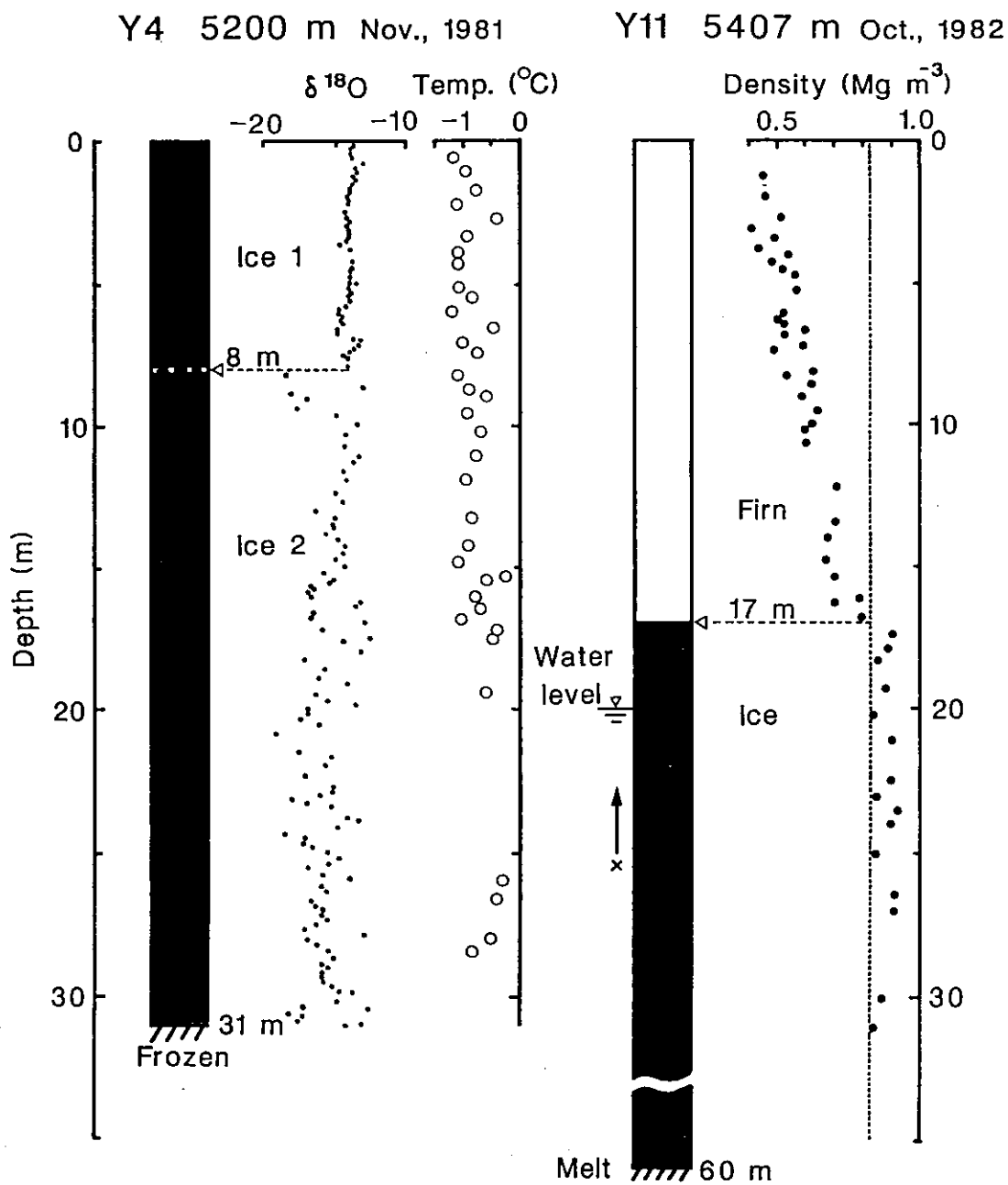


Fig. 4. Results of core analysis at Y4 (5200 m a.s.l.) and at Y11 (5407 m a.s.l.) on the Yala Glacier. After Watanabe et al. (1982, 1984).

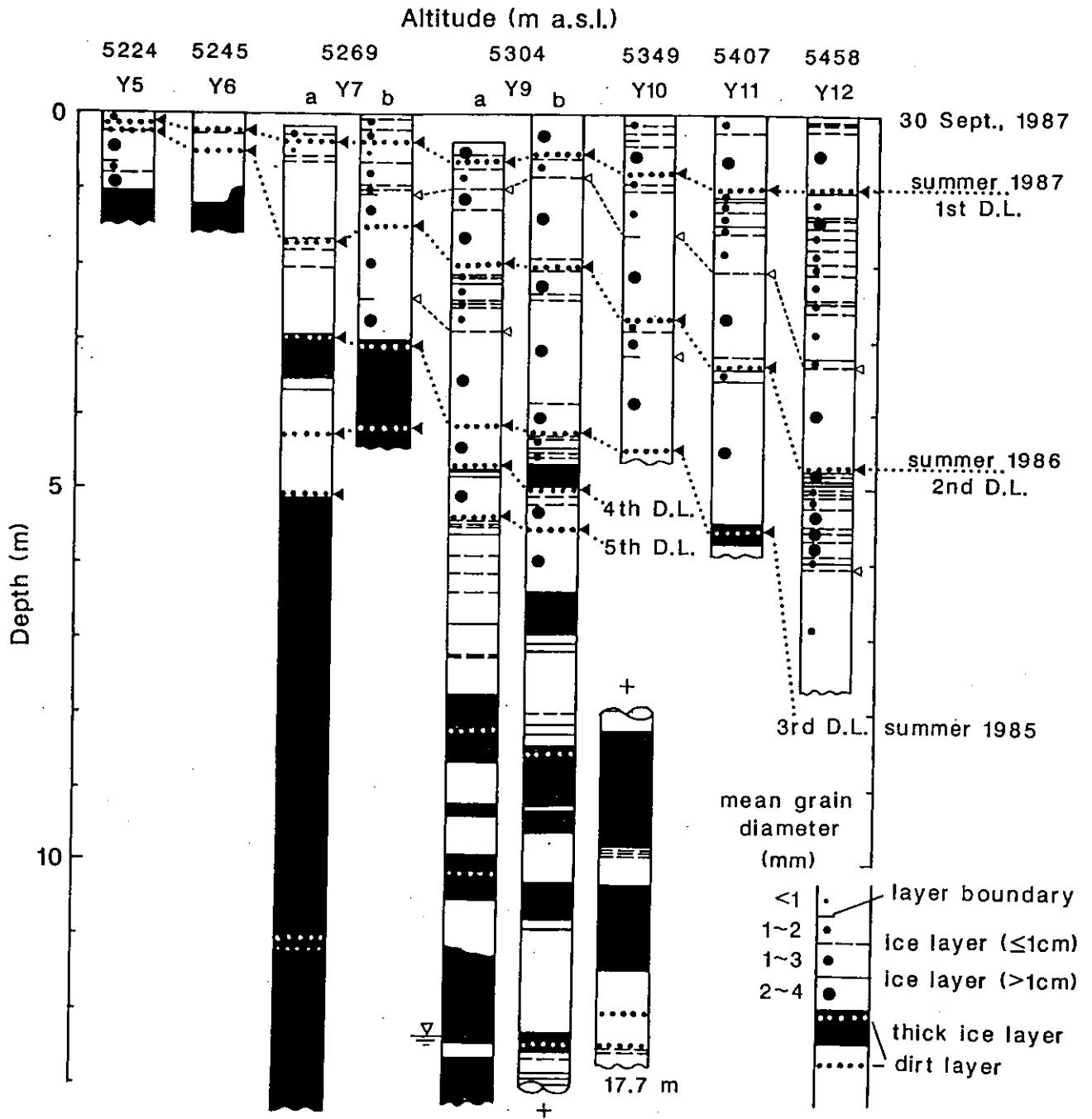


Fig. 5. Stratigraphic composition of ice and firn observed at seven sites in the accumulation area of the Yala Glacier. Black stripes represent ice layer and white parts represent permeable firn. The dotted line indicates position of dirt layer.

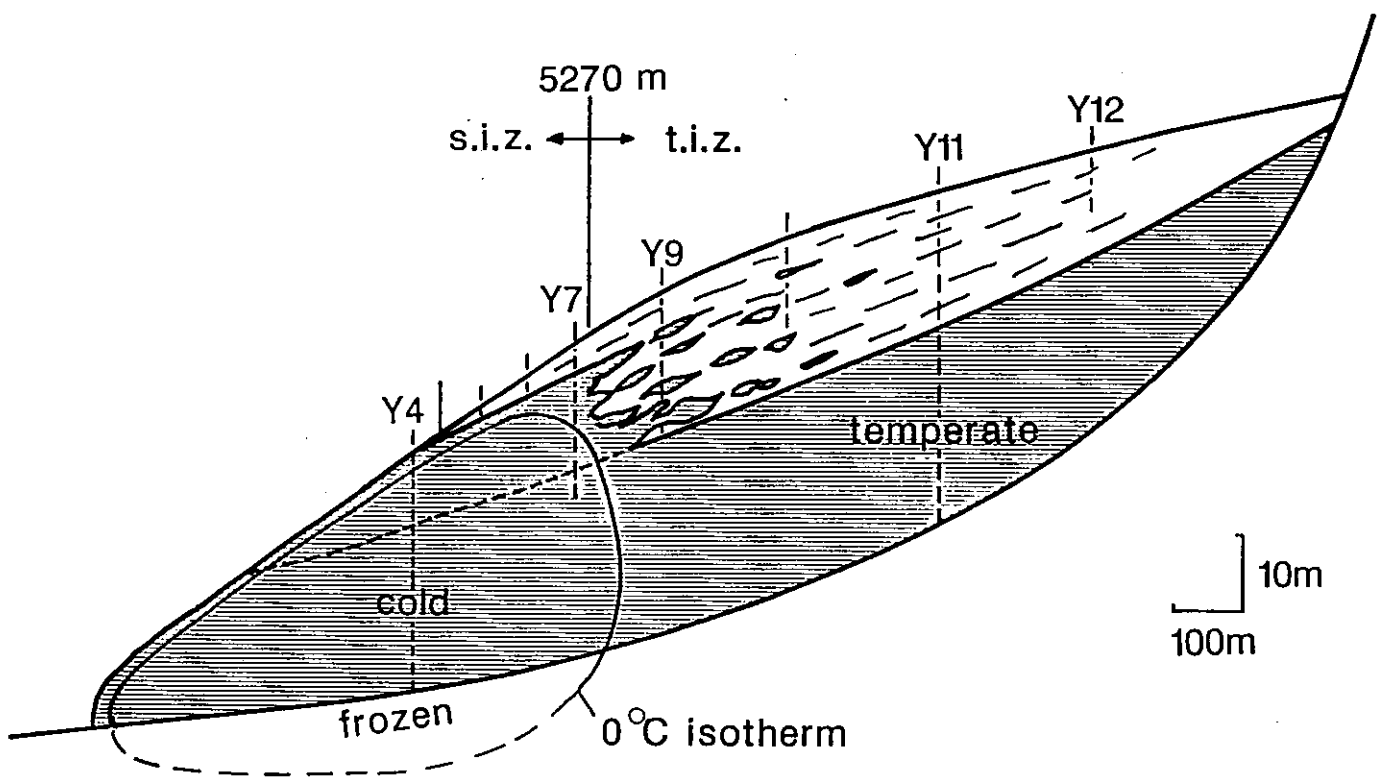


Fig. 6. Schematic illustration of the longitudinal section of the Yala Glacier.

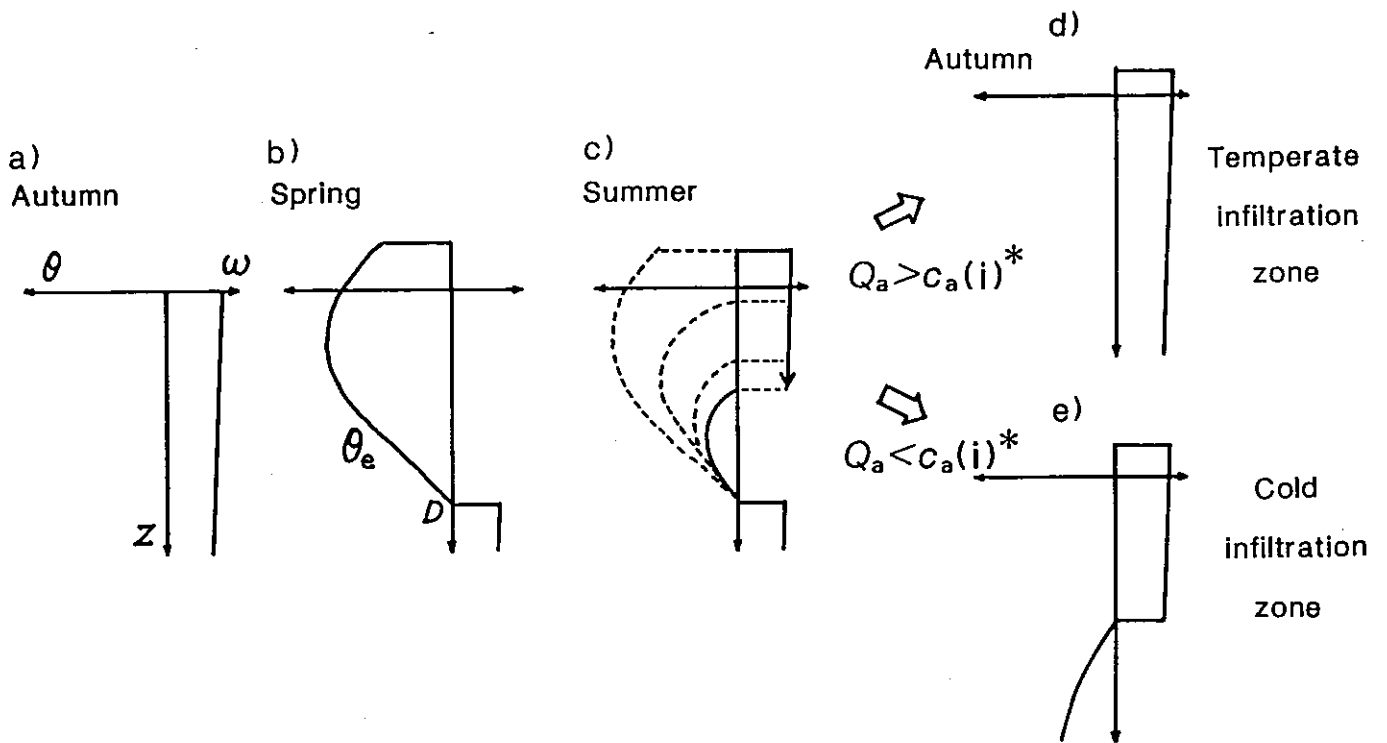


Fig. 7. Freezing process of wet firn and wetting process of the cooled firn during a year.

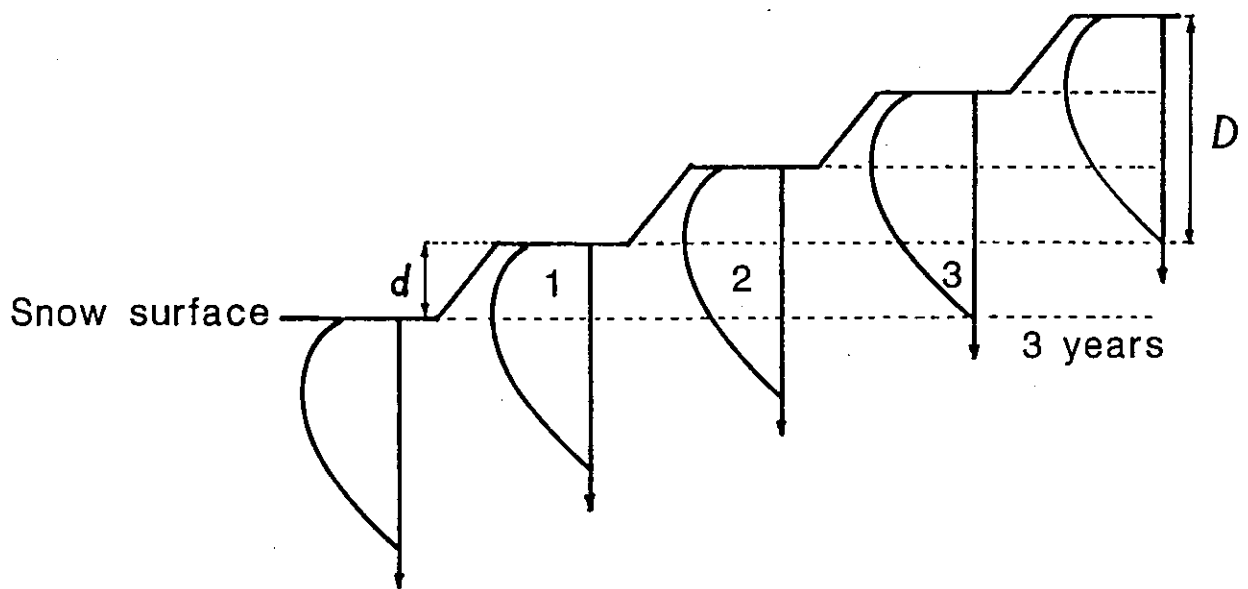


Fig. 8. Repeating process of the annual internal accumulation.

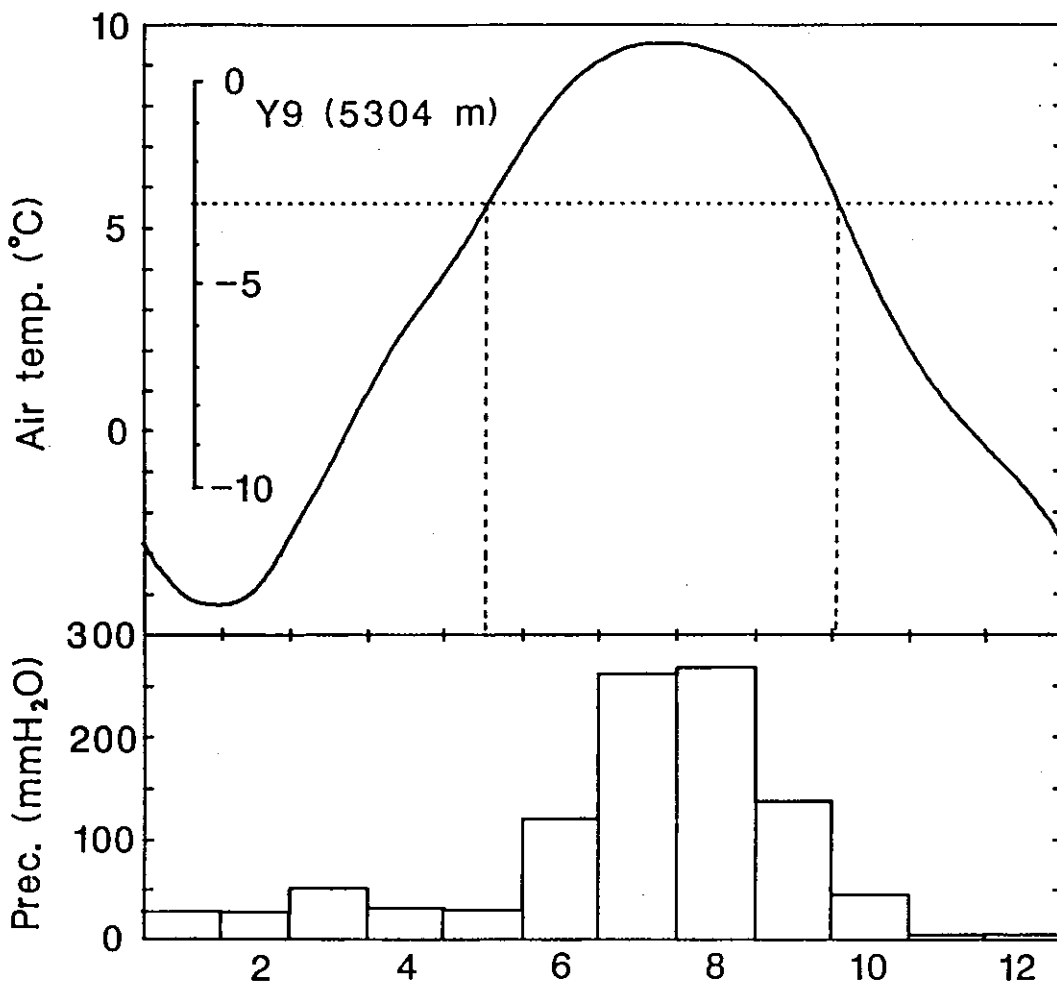


Fig. 9. Smoothed seasonal variation of air temperature and monthly precipitation at Kyangchen base house (BH, 3920 m a.s.l.). The annual precipitation is 1010 (mmH₂O).

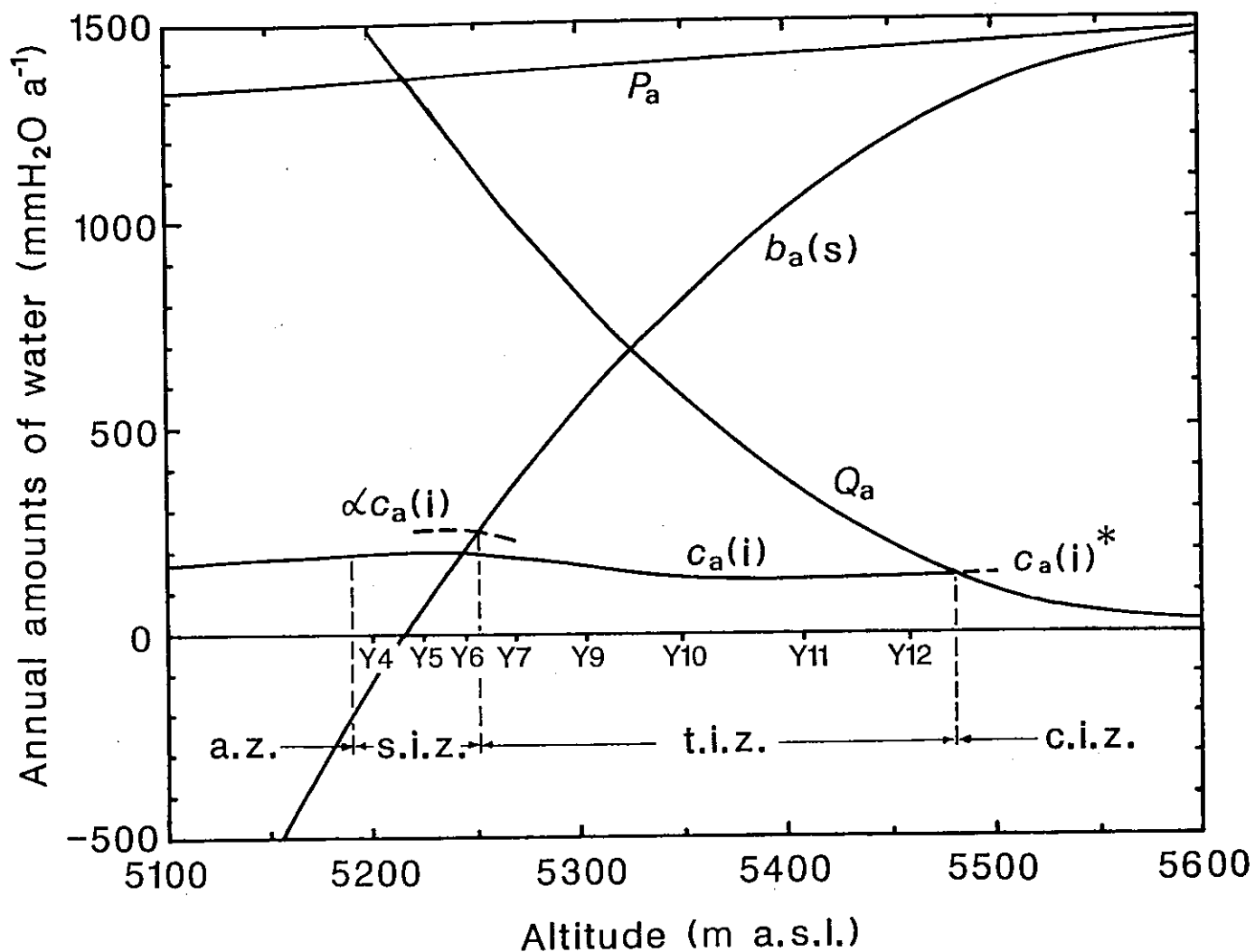


Fig. 10. Altitudinal distributions of annual amounts of water estimated on the Yala Glacier. $b_a(s)$: annual surface balance, Q_a : annual infiltration water, $c_a(i)$: annual internal accumulation, and P_a : annual precipitation. This glacier can be divided into following zones: cold infiltration zone (c.i.z.), temperate infiltration zone (t.i.z.), superimposed ice zone (s.i.z.) and cold ablation zone (a.z.).

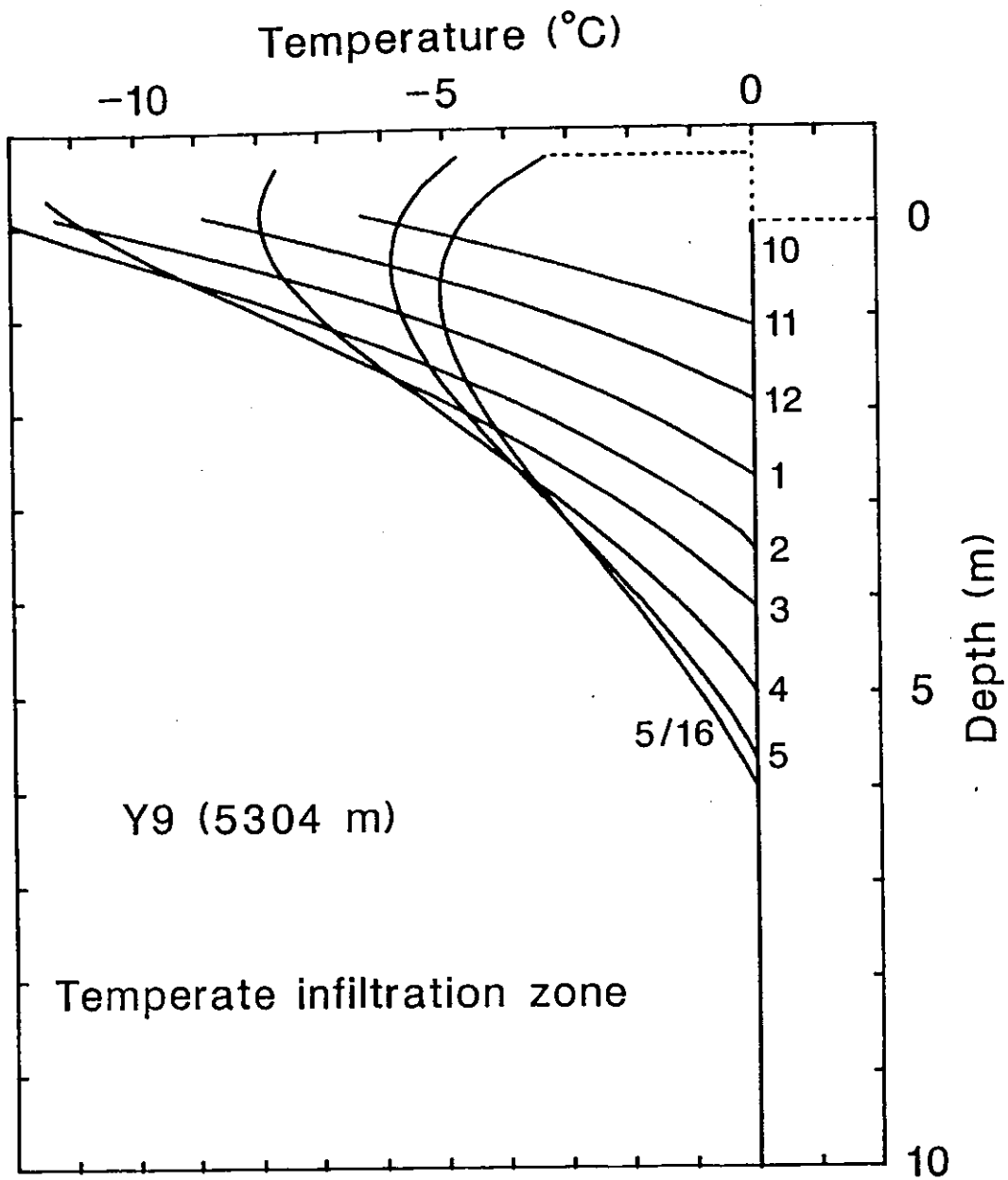


Fig. 11. Monthly variation of vertical profile of firn temperature calculated at Y9 in the temperate infiltration zone during winter (from 1st Oct. to 15th May.). The number denotes 1st of each month. The maximum freezing depth was 6 m.

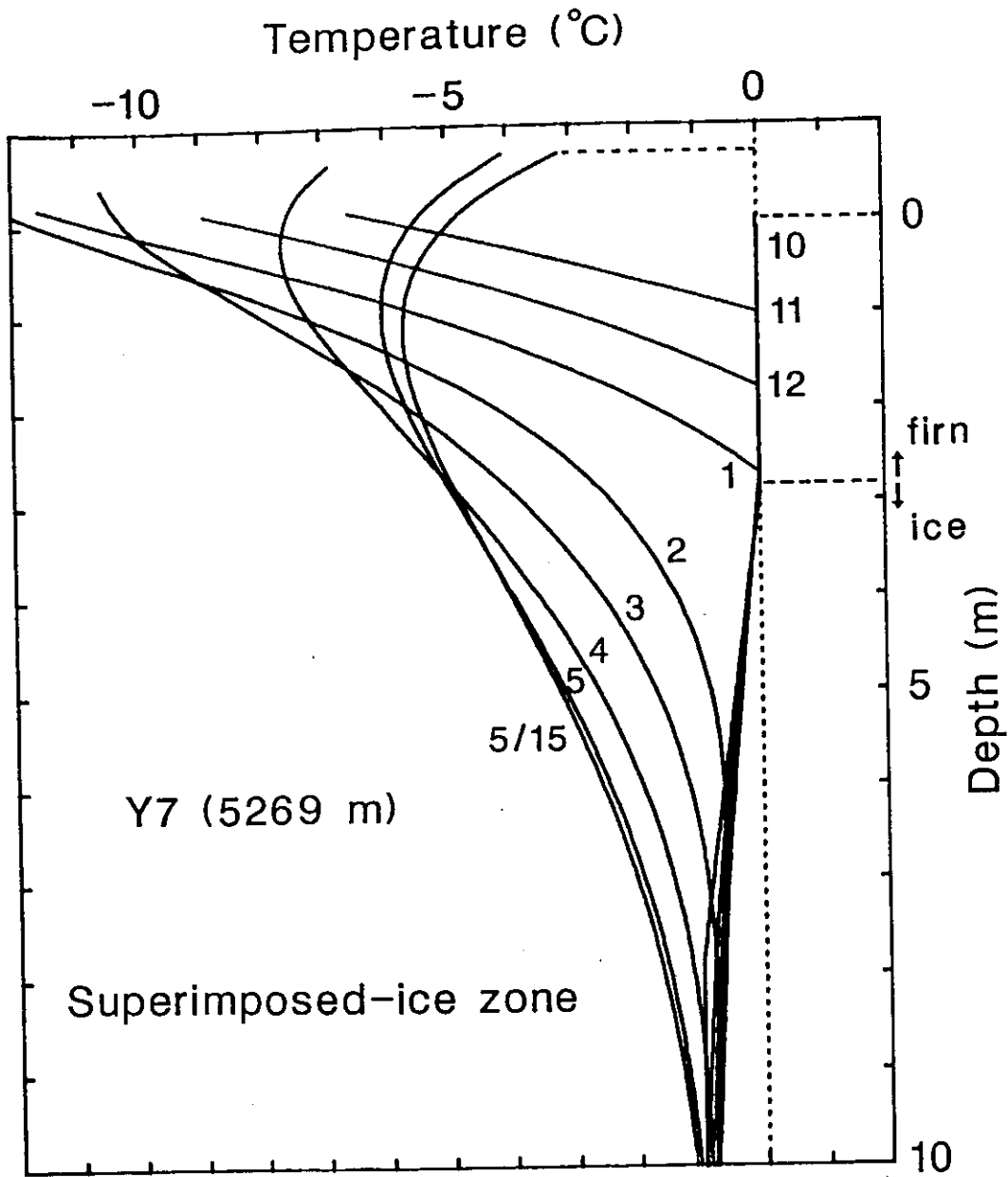
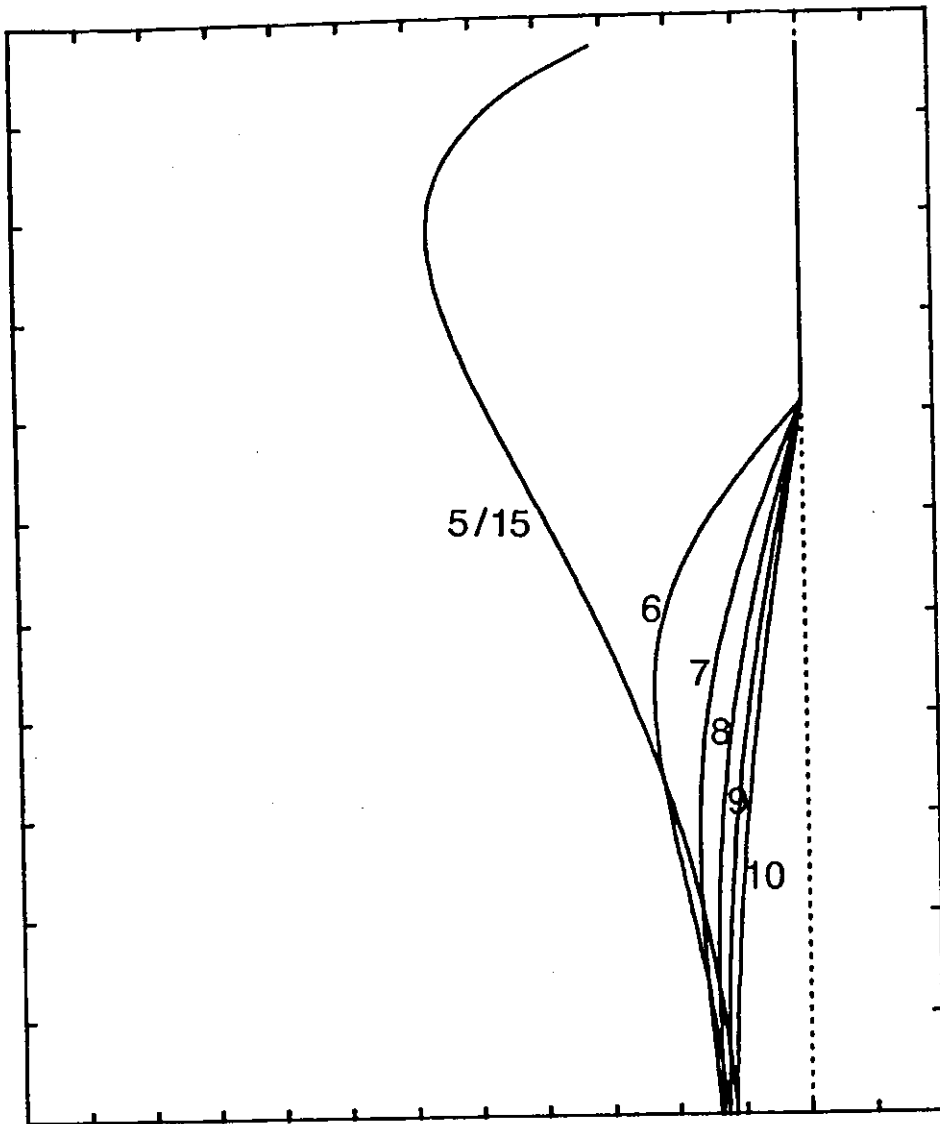


Fig. 12. Monthly variation of vertical profile of firn and ice temperature calculated at Y7 in the superimposed-ice zone.

(a): during winter (from 1st Oct. to 16th May.).



(b): during summer (from 16th May. to 1st Oct.).

The temperature at the isothermal depth (10 m) was -1°C .

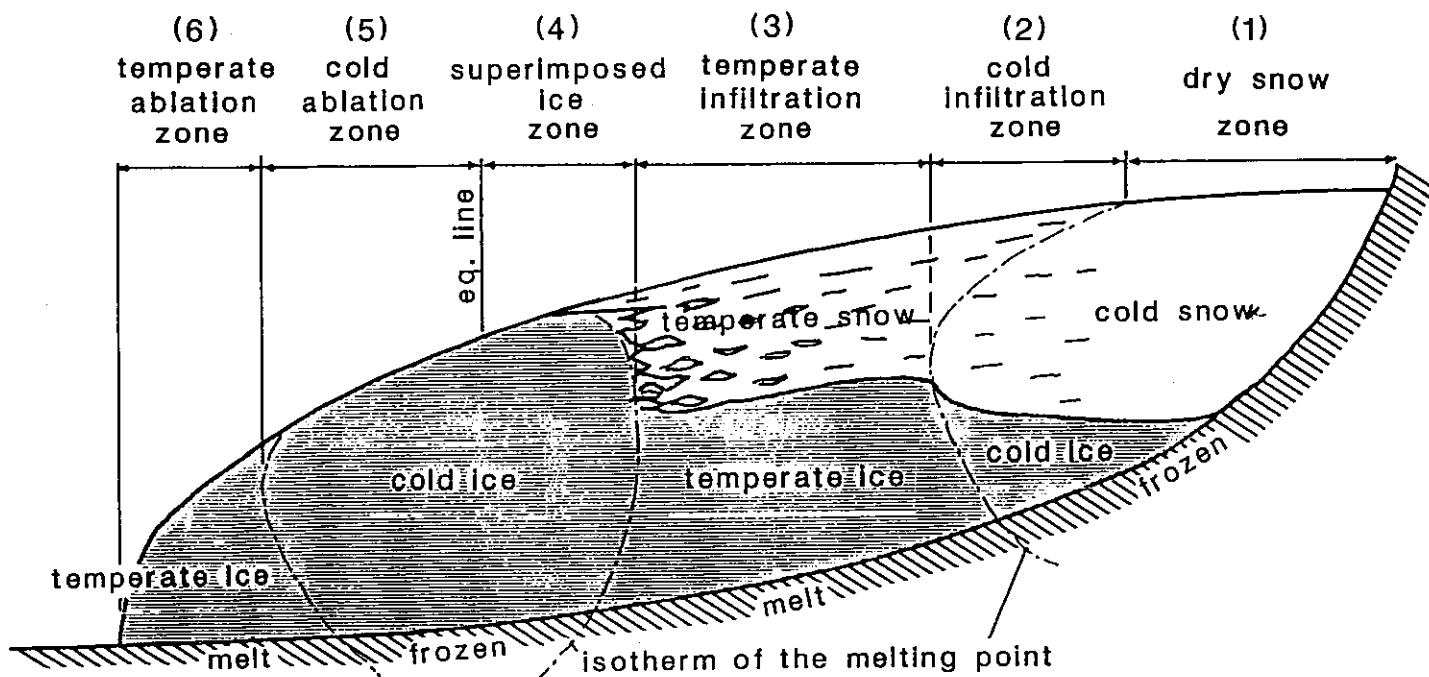


Fig. 13. An idealized glacier with six different thermal zones. The dash-dotted line represents the isotherm of the melting point in the end of summer.

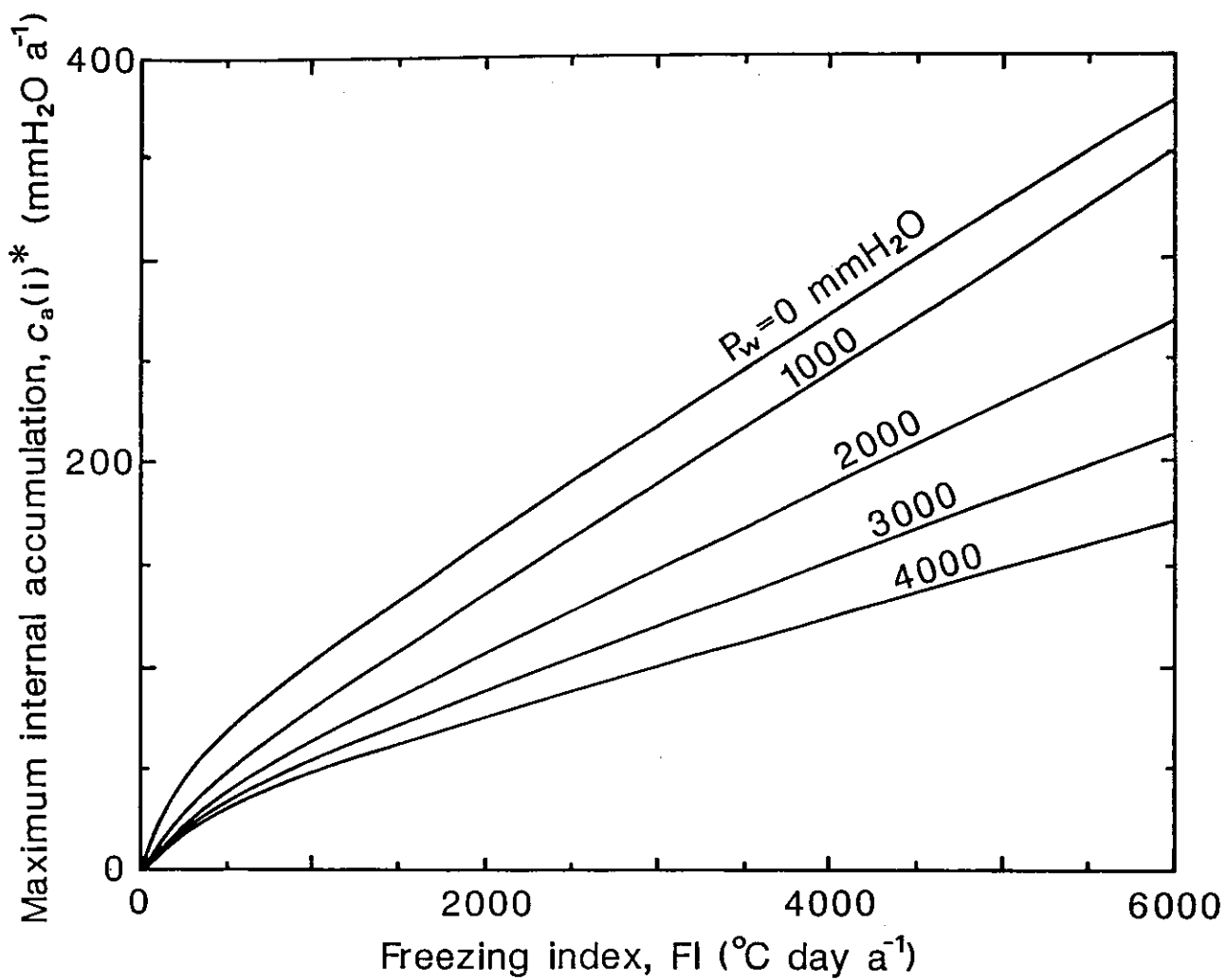


Fig. 14. Relationship among maximum internal accumulation and freezing index and winter precipitation.

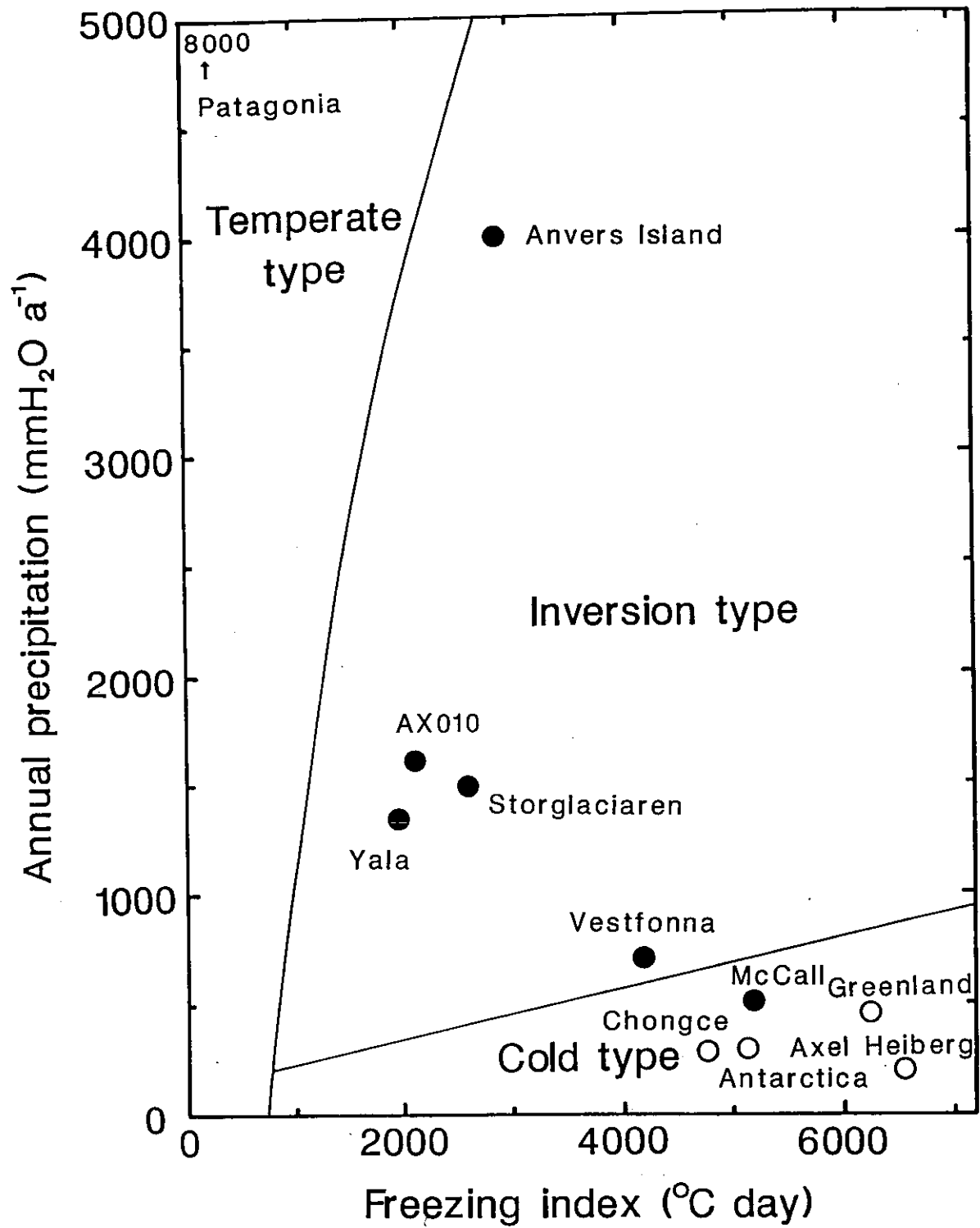


Fig. 15. Diagram showing three glacier types and climatic conditions (freezing index and annual precipitation).

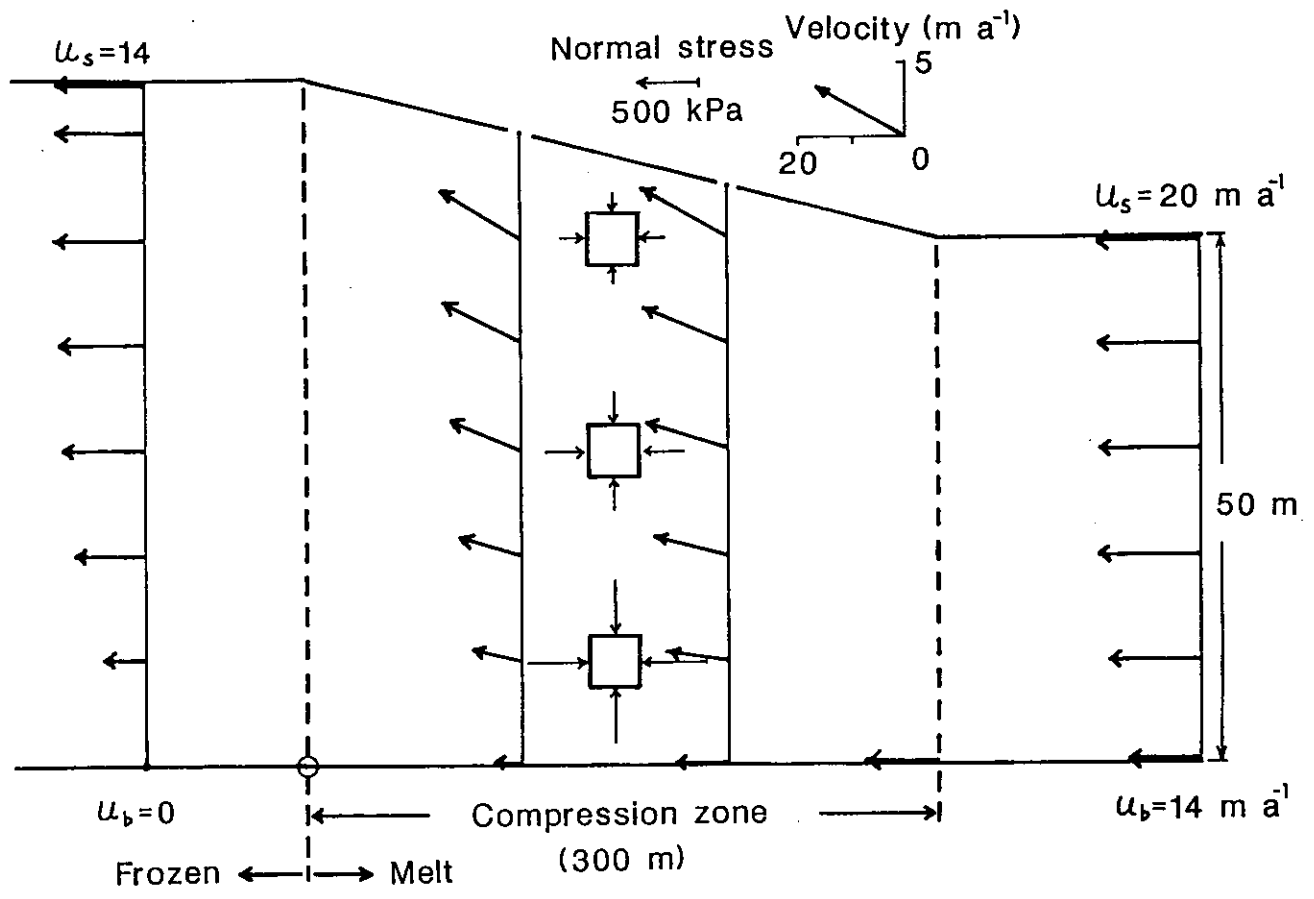


Fig. 16. Flow velocity and normal-stress components calculated in the transitional zone of the Yala Glacier.

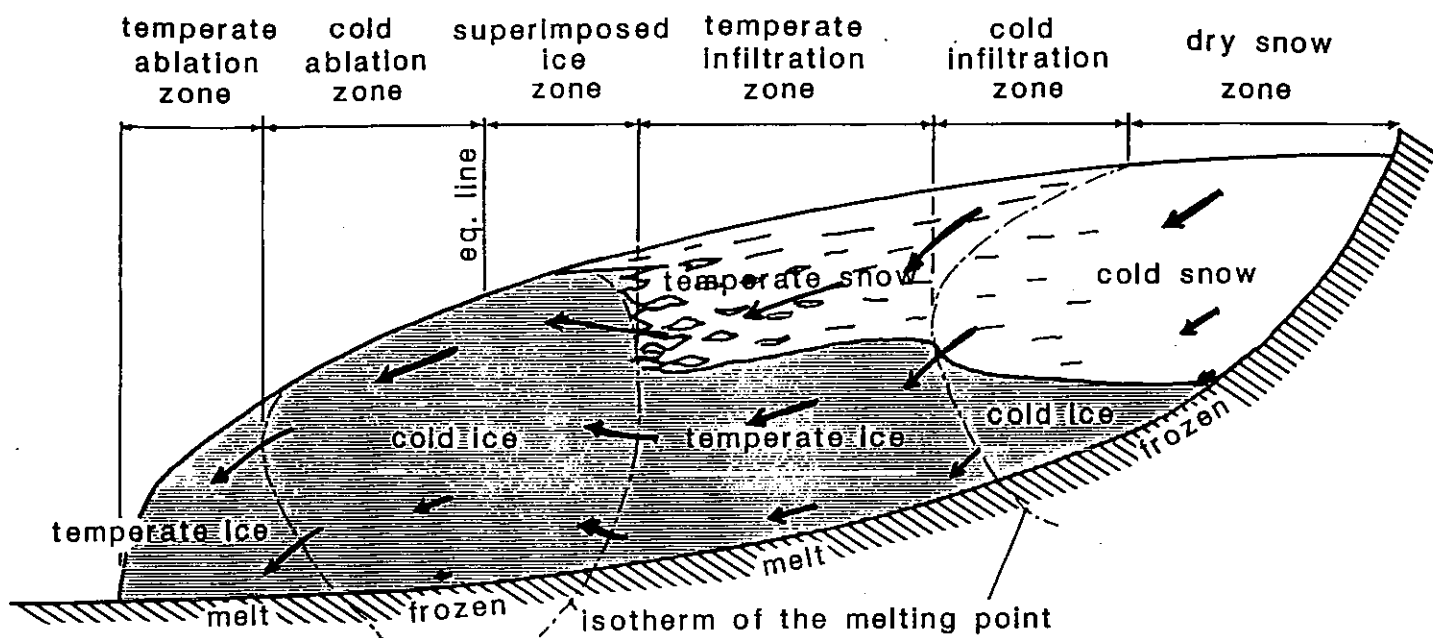


Fig. 17. Schematic flow lines estimated on the idealized glacier.

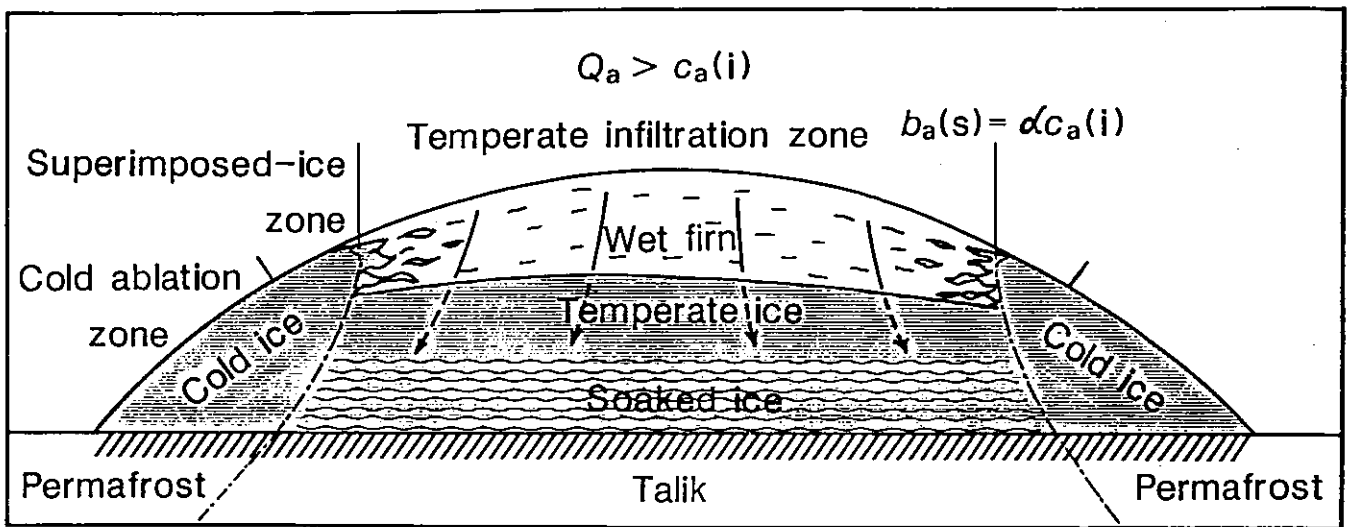


Fig. 18. The "water storage system" occurring in the inversion type glacier in the eastern Svalbard.